RESTRICTED INVESTIGATION REPORT 1638R

CSIRO

INSTITUTE OF ENERGY AND EARTH RESOURCES

DIVISION OF MINERAL PHYSICS AND MINERALOGY

MAGNETIC PROPERTIES OF THE BANDED-IRON FORMATIONS OF THE HAMERSLEY GROUP, W.A.

D.A. CLARK AND P.W. SCHMIDT

AMIRA PROJECT 78/P96B: APPLICATIONS OF ROCK MAGNETISM

PO Box 136
NORTH RYDE NSW
AUSTRALIA 2113

JUNE 1986

CSIRO

INSTITUTE OF ENERGY AND EARTH RESOURCES

DIVISION OF MINERAL PHYSICS AND MINERALOGY

POLICY ON RESTRICTED INVESTIGATION REPORTS

Restricted Investigation Reports issued by this Division deal with projects where CSIRO has been granted privileged access to research material. In return for this access, they provide recipients with an opportunity to take advantage of results obtained on their samples or problems. Initially, circulation of Restricted Investigation Reports is strictly controlled, and we treat them as confidential documents at this stage. They should not be quoted publicly, but may be referred to as a "personal communication" from the author(s) if my approval is sought and given beforehand.

The results embodied in a Restricted Investigation Report may eventually form part of a more widely circulated CSIRO publication. Agreements with sponsors or companies generally specify that drafts will be first submitted for their approval, to ensure that proprietary information of a confidential nature is not inadvertently included.

After a certain period of time, the confidentiality of particular Restricted Investigation Reports will no longer be an important issue. It may then be appropriate for CSIRO to announce the titles of such reports, and to allow inspection and copying by other persons. This procedure would disseminate information about CSIRO research more widely to Industry. However, it will not be applicable to all Restricted Investigation Reports. Proprietary interests of various kinds may require an extended period of confidentiality. Premature release of Restricted Investigation Reports arising from continuing collaborative projects (especially AMIRA projects) may also be undesirable, and a separate policy exists in such cases.

You are invited to express an opinion about the security status of the enclosed Restricted Investigation Report. Unless I hear to the contrary, I will assume that in eighteen months time I have your permission to place this Restricted Investigation Report on open file, when it will be generally available to interested persons for reading, making notes, or photocopying, as desired.

B.J.J. Embleton
CHIEF (Acting) OF DIVISION

August 1985

Distribution List

	Copy No.
AMIRA	1-17
CSIRO Division of Mineral Physics and Mineralogy	
D.A. Clark	18
P.W. Schmidt	19
B.J.J. Embleton	20
CSIRO IEER Records	21-24

This is copy number 19 of 24.

TABLE OF CONTENTS

LIST OF TABLES

LIST OF FIGURES

LIST OF APPENDICES

SUMMARY

This report describes the magnetic properties of rocks and iron ores of the Hamersley Group collected in and around the Tom Price and Paraburdoo mines. The availability of fresh orientable BIF samples from drill holes has, for the first time, allowed the nature of the remanence of the BIFs to be defined. The main results of the study are listed below:

1. All BIF samples are likely to be contaminated by palaeomagnetic noise owing to the presence of soft multidomain magnetite as the main carrier of NRM. Surface samples are affected by weathering, which reduces the susceptibility and the intensity of palaeomagnetically and petrophysically meaningful remanence components, and lightning, which produces intense spurious remanence components. Drill core samples are uncontaminated by surface effects but nevertheless are affected by palaeomagnetic noise of two types: IRMs pervading the whole sample, most probably produced by geological logging with a magnet, and piezomagnetic components produced by drilling and sawing, which are only carried by magnetite grains on the cut surfaces.

2. The palaeomagnetic noise carried by drill core BIF samples and some lightning-affected surface samples is readily removed by AF cleaning, at the expense of information regarding the original (uncontaminated) NRM intensity. Piezomagnetic components can be removed by soaking specimens in acid without affecting the other components. Original NRM intensities of AF cleaned specimens can be estimated by extrapolation of demagnetisation curves to zero field.

3. On the basis of palaeomagnetic cleaning experiments the representative in situ NRM of the Hamersley BIFs is interpreted to be dominated by an ancient (Proterozoic) component directed roughly NW with low negative (upward) inclination. Viscous remanence appears to be only a very minor component of the NRM. The cleaned remanence directions from the Dales Gorge and Joffre members at Paraburdoo and Wittenoom agree only after structural correction, constituting a positive fold test. This implies that the age of magnetisation pre-dates deformation

associated with the Ophthalmian orogeny (~ 1800 m.y.). Thus the remanence carried by the BIFs in these areas, which are of relatively low metamorphic grade, is probably an early diagenetic CRM dating from the precipitation of the magnetite. The characteristic remanence direction, after structural correction, is dec = 314°, inc = -5° (α_{95} = 6°).

4. The remanence of iron ore samples from Paraburdoo is very stable and is essentially monocomponent with a characteristic direction dec = 305°, inc = -23° (α_{95} = 8°) with respect to the present horizontal. Iron ore samples collected from the Tom Price deposit for this study exhibit much greater variability than the Paraburdoo samples. The remanence tends to be less stable, with a distributed blocking temperature spectrum, and some samples appear to possess multicomponent (reversed?) magnetisations. The characteristic cleaned direction, which appears to be post-folding, is dec = 309°, inc = -9° (α_{95} = 11°). This direction is quite different from that obtained in an earlier study, for which the deposit was presumably sampled at a higher level. The results are interpreted to indicate a discrete, relatively early, mineralising event at Paraburdoo, in contrast to Tom Price where mineralisation progressed for a considerable time during the Proterozoic roughly spanning the interval between the mineralising events at Paraburdoo and Mt Newman.

5. Low field thermomagnetic curves of samples of the BIFs, ores and the Hamersley surface are readily interpreted in terms of the magnetic minerals present, their approximate relative abundances, their grain size distribution and domain structure.

6. Representative <u>in situ</u> NRMs were estimated from analysis of the palaeomagnetic cleaning experiments and were combined <u>vectorially</u> to yield estimated formation mean NRM vectors. This procedure suppresses palaeomagnetic noise and combines remanence measurements weighted according to their intensity, in order to obtain an unbiased estimate of the bulk remanence of the rock unit. Similarly susceptibility ellipsoids of individual specimens were combined <u>tensorially</u> to calculate estimated formation mean susceptibility ellipsoids.

7. The iron ores, whilst appreciably magnetic by normal standards, are much more weakly magnetised than the BIFs. Ore from the Paraburdoo 4E deposit has remarkably uniform properties, whereas Tom Price ore is much more variable and somewhat more magnetic, reflecting the presence of small but variable quantities of magnetite. The ores exhibit a weak magnetic fabric with magnetic foliation parallel to bedding.

8. There is a serious sampling problem in determining the anisotropic susceptibility of BIFs. As a check on the measurements a theoretical model of the susceptibility of a BIF was developed and applied to the Dales Gorge member, which is the most thoroughly studied BIF unit in the Hamersley Group. Variations in properties are expected due to variable magnetite content and distribution. For the type section at Wittenoom the effective bulk susceptibility is expected to lie in the range 0.06 - 0.09 G/Oe with intrinsic anisotropy 2.4-5.6, corresponding to an effective anisotropy of 3.4 - 7.2 when self-demagnetisation is taken into account. Such high anisotropies greatly modify magnetic signatures over BIF units.

9. The magnetic properties of all fresh BIFs appear to be similar. The susceptibility parallel to bedding generally lies in the range 0.05 - 0.10 G/Oe with high intrinsic anisotropy (2-4). Remanence contributes significantly to the total magnetisation with Q values ranging from 0.5 to 3 with typical values of 1-2.

10. It is shown that the volume of BIF ($\sim$ 60,000 km^3) in the Hamersley Basin should produce an observable anomaly at satellite heights. The Basin is modelled as a thin rectangular plate and is assigned typical magnetic properties, based on this study. The theoretical anomaly at 400 km height has total amplitude $\sim$ 6 γ which corresponds well to the amplitude of the observed MAGSAT anomaly. Thus the BIFs probably constitute the main source of the MAGSAT anomaly over the Hamersley Basin and a deep crustal source is unnecessary.

11. Consideration of the anisotropy and remanence of the BIFs has allowed previously enigmatic magnetic signatures over mapped structures

to be satisfactorily explained. This implies that, armed with this essential information, magnetic surveys over buried features can now be interpreted with confidence in terms of geological structure. This analysis, which makes use of magnetic survey data supplied by Hamersley Exploration Ltd., is contained in a supplementary report which remains confidential to CRAE and Hamersley Exploration.

1. Introduction and Methods

The sites sampled for this project lie in the Tom Price and Paraburdoo mining areas of the Hamersley Basin, Western Australia. Forty two independently oriented block samples and 15 drill core samples were collected from the Tom Price area, while 30 block samples and 18 drill core samples were collected from the Paraburdoo area. Details of sampling are given in Appendix I. The Paraburdoo drill core samples were from four holes - 6 from DDH3 and 3 from DDH4 (Marra Mamba ore), 9 from DDH42 (fresh Dales Gorge Banded Iron Formation - BIF) and 13 from DDH44 (fresh Joffre and Weeli Wolli BIF). DDH42 and DDH44 were sampled to provide information on the magnetic properties of unaltered BIF. It is also possible to azimuthally orient these two cores using the consistent south dipping bedding attitude present throughout the Paraburdoo area. The procedure followed to orient the cores is dealt with in Appendix II. Several specimens (nominally 2.5 cm dia. x 2.2 cm ht.) were prepared from each individual sample to provide duplicate analyses. Each specimen was measured using a DIGICO balanced-fluxgate spinner magnetometer or a CTF cryogenic magnetometer for magnetic remanence. The CSIRO susceptibility bridge/furnace instrument (Ridley and Brown, 1980) or DIGICO susceptibility unit were used for bulk susceptibility and bulk susceptibility variation with temperature determinations and the DIGICO anisotropy (of susceptibility) delineator was used to determine magnetic fabric. Alternating field (AF) demagnetisation was effected using the CSIRO three axis tumbler or a Schonstedt GSD-1 demagnetiser, while the CSIRO non-magnetic furnace was used for step-wise thermal demagnetisation and the DIGICO fluxgate/high temperature rig was used for the continuous thermal demagnetisation work.

2. Remanent Magnetism

2.1 Drill Core Samples

Measured with respect to the apparent down dip azimuth, directions of natural remanent magnetisation (NRM) were generally scattered in all drill holes sampled except DDH44 (Fig. 1a,b). Directions from DDH44 group fairly well in one octant. The girdle distribution of directions

from DDH42 reflects the bedding plane attitude. Because of the anisotropy associated with the bedding and the high susceptibility, the observed magnetisations are constrained to the bedding plane. The origin of the scattering is not thought to be an intrinsic property of the BIF, but is probably induced during sample preparation (Appendix II) or perhaps during logging of the core when hand magnets are used to determine the presence of magnetite. Some samples displayed a good correlation between divergence from the mean direction and intensity. Intensities of some divergent samples were found to be as high as 0.3 G. These spurious magnetisations were demagnetised in fairly low AFs (50 Oe to 100 Oe), within the range of values typical of small permanent magnets. The effect of preliminary AF demagnetisation is presented in Fig. 2 where scattered magnetisations of various selected specimens from DDH42 are shown to converge towards the mean direction. Therefore the predominant magnetisation present in the fresh BIF at Paraburdoo has a consistent direction which appears to be carried by magnetite. AF cleaning of samples from DDH 3 and 4 either had little effect, or tended to further scatter magnetisation directions. Some samples from DDH 93 behaved similarly to DDH 42, cleaning up towards a common direction, but in many cases between-sample directions were scattered, probably due to difficulties in correctly orienting the samples in this structurally complex area.

Orthogonal projection representations (Schmidt and Clark, 1985) of demagnetisation behaviour of samples from DDH42 and DDH44 are given in Fig. 3, comparing both thermal and AF results. These examples are plotted with respect to specimen co-ordinates, prior to orientation. It is apparent that both techniques yield similar results (c.f. Fig. 3a and b, sample 44/49.8). Although complete demagnetisation is achieved only by thermal demagnetisation, the direction of magnetisation up to 300 Oe AF demagnetisation is similar for sample 44/49.8. Thermal demagnetisation is only achieved at 700°C indicating that haematite is the most stable magnetic carrier in this sample. Examples of results from applying cleaning to samples that displayed scattered NRM directions (from DDH42) are revealed in Figs. 3 c, e and f. Fig. 3e shows a dramatic reduction in intensity and change in direction of magnetisation

of sample 42/207.0C at an AF field of only 50 Oe. The remaining component (expanded in Fig. 3f) is almost parallel to components isolated after cleaning from other samples from DDH42 and 44. Fig. 3c gives results from a duplicate specimen from this same sample (42/207.0B) of thermal demagnetisation following AF (50 Oe) demagnetisation. This combined demagnetisation (AF followed by thermal) has been shown to be most efficacious when dealing with rocks whose remanences have been disturbed by strong magnetic fields (~ 50 Oe or larger) such as those accompanying lightning strikes (Schmidt and Embleton, 1985). This approach was adopted as a routine procedure, particularly for treating samples collected from natural outcrop which from experience are widely affected by lightning. The remaining example given (Fig. 3d) is from a sample of dolerite taken from DDH44. The intensity of magnetisation of this sample (44/174.8C) is relatively weak, but is similarly directed to those of the BIF samples.

Following magnetic cleaning, the component of magnetisation determined by linearity spectrum analysis (LSA - Schmidt and Clark, 1985) after drill core orientation (Appendix II) were in close agreement at D = 294.3°, I = -35.1° (α_{95} = 7.7°) for DDH42 and D = 290.5°, I = -42.2° (α_{95} = 8.7°) for DDH44. Table 1 lists these directions and their corresponding directions after a second correction has been applied to restore the directions to the palaeo-horizontal. Following bedding correction the directons are brought into even closer agreement, yielding an overall mean direction of magnetisation of D = 314.0°, I = -4.7° (α_{95} = 5.8°) and a corresponding palaeomagnetic pole position of Lat. = 40.9°S, Long. = 225.7°E (dp = 2.9°, dm = 5.8°). These results are discussed in relation to others below.

Samples from Paraburdoo DDH3 and DDH4 and Tom Price DDH 93/80 yielded scattered directions (Fig. 4 and Table 1) after applying LSA to the thermal (after AF) demagnetisation results. Although both DDH3 and DDH4 intersected Marra Mamba ore these scattered directions are probably not intrinsic to this formation but rather reflect intense weathering, both these holes being shallow (less than 100 m). In part, the scatter may also arise from orientation errors due to difficulty in defining the bedding planes. With such large errors it is not justified to carry out

the refined orienation correction as for DDH 42 and 44 where errors were much smaller. It is appropriate to assume that DDH3 and 4 do not depart widely from vertical (particularly since they are short) and use the general southerly dip as shown on supplied cross-sections to orient these cores approximately. Thus simply adding 180° to all measured declinations, the mean direction from eight samples is D = 335.3°, I = -16.9° (α_{95} = 36°). The remaining drill core, from Tom Price north deposit (ND93/80), also yielded scattered directions and again making the simplistic assumption that bedding at ND93/80 dips roughly to the south (as indicated on cross-sections), a mean magnetisation direction of D = 249.6, I = -5.1 (α_{95} = 22°) is determined.

A note of caution should be added at this point regarding the use of computer packages (such as LSA) as 'black-boxes'. In short they work correctly if, and only if, the assumptions made can be justified. If the wrong assumptions are made, LSA typically returns large errors and this is undoubtedly part of the problem with DDH 3,4 and 93. In addition, because the errors are probably no longer random, the calculated errors may be underestimated. For instance given the generally complex structures present at Tom Price it is doubtful if it is justifiable to assume a constant southerly dip on a small scale, even if cross-sections show a general large scale southerly dip. A closer inspecton of the samples showed that some bedding features were skewed even on the scale of 20mm. Eliminating results from these samples, and further rejecting results that appear to be outliers yields a direction for DDH 93 of about D=290°, I=-10°, not greatly dissimilar from the unaltered BIF core samples from Paraburdoo. This rather intriguing result suggests a similarity of the ages of mineralisation (ND93/80 being mainly mineralised) and BIF formation. This relationship is reinforced by the results from the pits at Paraburdoo and Tom Price and is further elaborated upon below.

2.2 Oriented Block Samples

All surface samples from the mines and surrounds were oriented using the sun compass/clinometer device and/or a magnetic compass. When both methods are used it is possible to detect any anomalous local

magnetic field present at the sampling site. Local declination anomalies at the sampling sites are listed in Appendix III. Deflections in declination of the compass needle were very pronounced around natural outcrops, particularly at Mt Nameless (near Tom Price), strongly suggesting the effects of lightning. This, plus the effects of weathering have combined to give very scattered results for samples collected from natural outcrops.

The size of the declination anomalies observed near strongly magnetised rocks demonstrates the possible errors in drill hole surveys which rely on magnetic bearings, in the vicinity of BIF. Although sub-surface BIFs are not affected by lighting they are much less oxidised and are inherently more magnetic than outcropping BIF.

Even when the sites with magnetic rocks are eliminated from the analysis, significant declination anomalies, which appear to be fairly consistent over the mine area, are apparent. The magnetic anomalies arising from the overall distribution of magnetic units are producing small but significant departures from the regional declination expected for the Hamersley province. Over the Tom Price deposit the compass needle is deflected 3°W on average, and at Paraburdoo the average declination anomaly is 3°E.

Fig. 5 displays directions of NRM of all specimens from surface samples collected. Although directions are scattered (particularly those from Tom Price, reflecting the contribution of samples from Mt Nameless) there is a clear tendency to group in the northwest-up octant, similar to the directions from the fresh BIF at Paraburdoo.

In areas of widespread evidence of the effects of lightning the most efficaceous cleaning technique has been found to be thermal cleaning following preliminary AF cleaning (Schmidt and Embleton 1985). This procedure was used here with AF cleaning to 20 or 30 mT, followed by thermal cleaning to the Curie point. Representative demagnetisation behaviour for surface samples from Paraburdoo is displayed in Fig. 6. Both directions and intensities of most samples are very stable and the magnetisations only decrease after heating to

just below the Curie temperature. Typically samples show a single component of magnetisation although one sample (Fig. 6f) reveals multicomponent magnetisation. This complicated magnetic signature is found in samples of the Wyloo Conglomerate, and suggests that the magnetisation of the individual ore clasts forming the conglomerate predates deposition of the conglomerate. Each measurement of the magnetisation of such a sample would simply be the resultant of the magnetisation of each constituent (clasts plus matrix). This is discussed further below, in the context of the possible age of formation of the ore. Other samples displaying aberrant behaviour came from sites 05, 06 and 08. Samples from site 08 appeared to be very weathered and yielded directions close to the Tertiary (normal and reversed) field (Fig. 7a) while both sites 05 and 06 were from the Marra Mamba member which is also weathered and may contain Tertiary magnetic components. These samples are scattered and have been eliminated for the purpose of calculating a mean direction of magnetisation. Sample directions following LSA are plotted in Fig. 7a. A mean direction from 15 samples (excluding those from the Wyloo conglomerate) was determined with D = 304.7°, I = -23.0° (α_{95} = 8.3°).

The orthogonal plots in Fig. 8 show representative demagnetisation behaviour of surface samples from Tom Price (excluding those from natural outcrop). These samples are not as stable as those from Paraburdoo although their stabilty is by no means low. In fact the main difference between the Paraburdoo and Tom Price samples is that the latter possess a broad spectrum of unblocking temperatures as opposed to the narrow or discrete unblocking temperatures displayed by the Paraburdoo samples. With regard to the directions of magnetisations it is apparent that most are northwest-up, although one sample (TP05B1) is magnetised to the southeast-up (Fig. 8c) suggesting the presence of magnetic reversals. On closer inspection it is apparent that the demagnetisation trajectory of sample TP05B1 is not decaying towards the origin, but is heading from the southeast-up octant towards the northwest-up octant, which is further evidence for the presence of other components of magnetisation, possibly almost reversed. Much of the scatter of NRM directions found at Tom Price (Fig. 5a) might arise from

the presence of reversed magnetisations within a single specimen. Reappraising Fig. 5a there does appear to be a bimodal distribution present which supports the above contention. Sample directions following LSA are plotted in Fig. 7b. A mean direction from 19 samples of D = 308.8°, I = -9.3° (α_{95} = 11.2°) was determined for the samples from Tom Price excluding those from natural outcrop and several other directions suspected of possessing reversed components.

2.3 Discussion of Remanent Magnetisation

Previous work by Embleton et al (1979) on the Hamersley BIF from Wittenoom yielded results similar to those from BIF given here in Table 1. Combining the results from the Wittenoom BIF DDH47A and DDH51 (Appendix 2 - Embleton et al, 1979) yields a mean direction of D = 307.5°, I = -10.5° (α_{95} = 9°) from 20 samples. Following correction for bedding attitudes of 56° and 60° dips to the south for the Paraburdoo BIF DDH42 and DDH44, respectively, yields a direction of D = 314.0°, I = -4.7° (α_{95} = 6°) as given in Table 1 which is indistinguishable from the Wittenoom BIF direction. Sample directions from DDH42 and DDH44 are plotted in Fig. 9a and their mean direction both before and after bedding correction is compared with the Wittenoom BIF direction in Fig. 9b. The agreement is clearly much better after bedding correction, implying that the magnetisation pre-dates the time of folding. Applying the statistical fold test devised by McFadden and Jones (1981) a common true mean direction for the Wittenoom and Paraburdoo BIFs is rejected with 99^{+}% confidence in their present-day attitudes, but can not be rejected (at 99^{+}% confidence) after returning the Paraburdoo mean magnetisation direction to the palaeo-horizontal. Thus not only does the BIF possess a consistent magnetisation direction, the magnetisation probably dates from the time of formation, and is certainly pre-folding in age. In principle the measured inclinations should be corrected for the anisotropy of the BIF specimens. The correction is quite small, however, because of the low palaeolatitude and does not alter the conclusions.

Also plotted in Fig. 9b are the mean directions from the surface samples (Table 1), both before and after folding. For both the

Paraburdoo samples (PB) and the Tom Price samples (TP) internal scatter increases slightly after correcting for bedding attitudes (including plunging at Tom Price), suggesting that the magnetisation may be post-folding (Table 1). However the increased dispersion of the Paraburdoo directions is slight because of the consistency of structural attitudes at the sampling sites. The similarity of the pre-folding directions from the BIFs and the directions from the Paraburdoo ore samples strongly suggests that the time of mineralisation (at Paraburdoo at least) must have followed fairly closely the time of BIF formation.

The picture is not so clear cut at Tom Price where the mean direction of the surface samples appears to be in better agreement with the BIF direction in their present attitudes. The increase in dispersion of the Tom Price directions after restoring bedding to the horizontal (Table 1) also suggests that these magnetisations are post-folding. The directions we have found are, however, quite different from those found previously at Tom Price (Porath and Chamalaun, 1968). The ore forming processes at Tom Price appear to have involved a greater length of time than those at Paraburdoo, with magnetic reversals being recorded (Fig. 7b) and considerable changes in the local magnetic field axis probably reflecting changes in latitude while the ore forming processes were active. If we assume that the northwest-up directions found here are north-seeking then the samples collected for this study were magnetised in low southern hemisphere latitudes, while those collected by Porath and Chamalaun (1968) appear to have been magnetised in northern hemisphere latitudes. If the polarity assumption is reversed then so too are the palaeolatitudes but the main point is the great length of time covered by the period of mineralisation. The mean direction quoted by Porath and Chamalaun (1968) from Tom Price is D = 304°, I = 25° (α_{95} = 12°), which is significantly different from the direction determined here (Table 1) even considering the fairly large cones of confidence from the two studies. The large dispersion of the Tom Price directions relative to other results (Table 1 and from Mt Newman in Porath and Chamalaun, 1968) may be attributed, in part, to continental drift although the presence of reversals is also possibly also instrumental.

The mean direction quoted by Porath and Chamalaun (1968) from Mt Newman is D = 302°, I = 39° (α_{95} = 9.5°) which is supported by an unpublished result of ours, albeit from only three samples, with D = 308°, I = 50° (α_{95} = 8°), indicating magnetisation in mid northern latitudes (making the same assumption regarding polarity as above). There is no indication of the presence of magnetic reversals at Mt Newman, suggesting the mineralising event there was short.

2.4 Summary of Remanent Magnetisation

Following AF and thermal cleaning of samples of fresh BIF, oxidised BIF and iron ore of varying grades, a self-consistent picture has emerged regarding the timing of the transformation from BIF to ore. The pre-folding magnetisation (probably original chemical remanent magnetisation) direction of the BIF is now well established indicating that equatorial latitudes prevailed during deposition (c.f. high latitudes during Fortescue times, Fig. 10 - Schmidt and Embleton, 1985). Magnetisations of oxidised BIF and ore from Paraburdoo appear to date from shortly after deposition of the BIF and before the orogeny which deformed them. The ore forming processes at Tom Price were probably initiated at similar times as those at Paraburdoo but proceeded long afterwards since magnetic reversals and a considerable range of palaeo-latitudes are recorded at Tom Price. There may have been two distinct episodes of mineralisation at Tom Price although further work would be required to investigate this. The mineralisation at Mt Newman appears to have occurred at a similar time as the late stages of enrichment at Tom Price.

3. Rock Magnetic Properties

3.1 Low-field thermomagnetic curves

Thermomagnetic analysis of representative samples of different lithologies was carried out in order to define the magnetic minerals present and to estimate relative contributions of different mineral species to the magnetic properties of the rocks and ores. The susceptibility of small crushed sub-samples was continuously monitored as a function of temperature between -200°C and 700°C. The resulting

k-T curves are shown in Fig. 12.

In order to interpret these curves a knowledge of the various magnetic transitions exhibited by magnetic iron oxides is necessary. All magnetic minerals are characterised by a Curie point, which is dependent on composition, below which they exhibit magnetic order (ferromagnetism or ferrimagnetism) and therefore have relatively high susceptibility, and above which they are paramagnetic with very low susceptibility. On the k-T curves the Curie point is marked by a very steep descent to a plateau value which is nearly zero. The Curie temperature is ~ 580°C for pure magnetite and ~ 680°C for pure haematite.

Magnetite also exhibits a well-defined peak in susceptibility at ~ -155°C, the isotropic point. This marks the temperature at which the first magnetocrystalline anisotropy constant K_1 passes through zero ($K_1 > 0$ below the isotropic point, $K_1 < 0$ above the isotropic point). The susceptibility peak is very sensitive to stoichiometry in multidomain grains and is also suppressed in assemblages of single domain grains, which are dominated by shape anisotropy of inequidimensional grains rather than by magnetocrystalline anisotropy. A prominent peak at ~ -155°C therefore indicates nearly pure multidomain magnetite.

At low temperatures haematite is perfectly antiferromagnetic, apart from effects due to crystal defects, with spins lying along the c-axis. At the Morin transition, which occurs at ~ -10°C, the spins flip into the basal plane and the two spin sub-lattices depart slightly from antiparallelism producing a weak ferromagnetic moment within the basal plane. This transition is marked by a relatively sudden rise in susceptibility as the haematite-bearing specimen warms through the transition temperature.

At high temperatures fine magnetic grains exhibit marked increases in susceptibility curves immediately before the rapid drop to the Curie point. These so-called Hopkinson peaks are due to unblocking of the grains. As the grains, which are magnetically stable at ambient temperatures, pass through their unblocking temperatures they become

superparamagnetic, with greatly enhanced susceptibility until just below the Curie point. These unblocking peaks are greatly suppressed for multidomain grains, as the susceptibility is limited by self-demagnetisation in such grains.

Having briefly discussed the diagnostic features of k-T curves, the results presented in Fig. 12. can be interpreted. For example fresh BIF sample 300.5 m from Paraburdoo DDH 42, is a "type" curve for multidomain stoichiometric magnetite with a prominent isotropic point (a) and a Curie temperature of 580°C (points marked c in this Figure indicate the start of the rapid descent to the Curie point). The coincidence of heating and cooling curves (i.e. reversibility of the k-T curve) indicates that the observed behaviour reflects only magnetic phenomena and that chemical changes are imperceptible. The curve demonstrates that contributions to magnetic properties from other magnetic minerals are negligible.

The behaviour of a sample of Mt Newman ore (MNOIB) is much more complicated but is nevertheless readily interpretable. The susceptibility of unheated ore at ambient temperatures is due, in approximately equal measure, to haematite and to fine-grained magnetite. Of course magnetite is much less important volumetrically, because of its much higher specific susceptibility, and it probably occurs as small unoxidised cores within martite grains. At the Morin transition (b) there is an increase in total susceptibility due to the appearance of weak ferromagnetism in haematite. Above 400°C there is a spectacular unblocking peak associated with fine-grained magnetite. The contribution due to magnetite vanishes above the magnetite Curie point, leaving the contribution of haematite, which in turn disappears at 680°C. The irreversibility of the k-T curve on cooling indicates chemical change has taken place at high temperatures, with the production of extra magnetite approximately doubling the original (very small) fraction of magnetite in the sample.

Oxidised Dales Gorge BIF (TP01B) from the synclines deposit, Tom Price shows the contribution of magnetite and haematite to the susceptibility. Although magnetite is only a minor component of the

rock it dominates the magnetic properties due to its large specific susceptibility. In this case the magnetite is more coarse-grained than for the Mt Newman ore sample, as evidenced by the isotropic point (a) and the lack of an unblocking peak at high temperatures. The irreversibility of the curves (smaller signal on cooling) shows that some magnetite and haematite have been destroyed by heating. The non-magnetic phase which must have been produced is not known.

The magnetic ore from the Channar deposit has a fully reversible k-T curve which clearly indicates that the magnetic properties are dominated by a small fraction of multidomain magnetite (note the isotropic point and relatively flat curve up to the magnetite Curie point). Approximately 4% of the room temperature susceptibility is contributed by the volumetrically dominant but weakly magnetic microplaty haematite. Petrographic examination of Channar ore reveals that magnetite occurs as remnant cores within martite.

Paraburdoo H2M ore from the 4E deposit (PB01B) contains no magnetite. The reversible k-T curve exhibits a sudden rise in susceptibility, from a very low value, at the Morin transition and a Curie temperature of 680°C. The Hopkinson peak indicates unblocking temperatures in the approximate range 500-650°C, suggesting that this ore should be a reliable palaeomagnetic recorder.

The magnetic Canga sample exhibits a steady increase of susceptibility with temperature from -200°C up to ~ 580°C, with a Curie point just above 600°C. There is no sign of an isotropic point. This type of k-T curve typifies weathered profiles containing fine-grained, cation-deficient magnetite ("kenomagnetite"). The wide spectrum of unblocking temperatures indicates the presence of a grain fraction which is superparamagnetic at ambient temperatures and is likely to be associated with anomalous TEM response. A sample of relatively weakly magnetic Canga was shown to contain a lower proportion of multidomain stoichiometric magnetite, with a perceptible contribution to the susceptibility from a volumetrically dominant proportion of haematite.

3.2 Magnetic Petrophysics

The ultimate goal of this study was to provide estimates of representative magnetic properties of the BIF units and areas as an aid to magnetic interpretation. Particular questions which are addressed in this work include:

(i) the relative contributions of induced and remanent magnetisation to observed anomalies.

(ii) the presence or absence of a consistent remanence direction, oblique to the present field, in the BIFs and ores, and whether any such ancient remanence is pre-, syn- or post-folding.

(iii) the influence of susceptibility anisotropy and geological structure on the amplitude and form of anomalies associated with BIFs.

(iv) the possibility that the prominent MAGSAT anomaly observed over the Hamersley basin arises from the BIFs of the Hamersley group and not from a deep crustal feature.

Banded-iron formations are notoriously difficult to study and previous studies have shown that the remanence carried by outcropping BIF units is very complex and difficult to interpret. The availability of drill core from fresh BIF units has allowed determination of representative NRMs of BIF samples, uncontaminated by the effects of lightning and weathering, for the first time. This has also allowed an assessment of the efficacy of palaeomagnetic cleaning techniques in removing unrepresentative palaeomagnetic noise due to surface effects.

As discussed in Section 2, the raw NRM of the BIF samples and most of the ore samples consists essentially of a stable ancient component, directed NW with shallow negative inclination, overprinted to varying degrees by soft components with no consistent orientation. The soft components are interpreted as IRM "noise" due predominantly to lightning, in the case of surface samples, or to cultural effects, in the case of the drill-core samples. These soft components are therefore unrepresentative of the *in situ* magnetisation of the samples and must be discounted from the measured NRMs before combining measurements to yield an estimated formation mean remanence vector.

With few exceptions, there is little evidence of a significant VRM component in these samples, including those which are not contaminated with IRM noise. The approach taken to estimate the original monocomponent NRM in the fresh BIF samples was to determine the lowest AF step for which the IRM was totally removed, taking the AF-cleaned direction as the original NRM direction. The original NRM intensity was estimated by linear extrapolation to zero field of the residual intensity vs cleaning field relationship for the ancient components in the low field region.

Linear extrapolation is a reasonable procedure, based on extensive experience with AF demagnetisation of remanence carried by multidomain magnetite, as well as an approximately linear initial decay of intensity of the stable component with cleaning field observed for many of the specimens. Without such extrapolation the NRM intensity would be underestimated, typically by about 40% for DDH 42, because the original contribution of the soft (but nevertheless stable) grains to the NRM, before they were reprinted by an applied field, would be neglected. On the other hand, simply averaging the raw NRM intensities without regard to the direction or nature of the magnetisation would overestimate the in situ NRM in DDH 42 by 150%. The samples from DDH 44 were less contaminated in general and the corrections required were correspondingly less.

The relative simplicity of the NRM carried by unoxidised BIF and by most of the ores contrasts with the results obtained from outcropping BIF units. Knowledge of the characteristic remanence of the BIFs and ores, however enables recognition of spurious remanence components in surface samples by their odd directions. Moderate weathering of unoxidised BIF should reduce both the susceptibility and remanence as magnetite alters to haematite. However the remanence direction should remain unchanged as long as even a small fraction of unoxidised magnetite remains to dominate the NRM. Eventually complete oxidation of the magnetite should produce weak NRMs similar to those of Tertiary laterites, with scattered normal and reversed groups plus many intermediate directions.

The bulk susceptibilities, NRM vectors and Koenigsberger ratios of samples collected from the open pits and natural outcrops at Paraburdoo and Tom Price are listed in Tables 3 and 4 respectively.

The quoted sample NRMs are vector means, i.e. vector sums of the NRMs of the specimens cut from them, divided by the number of specimens. This procedure yields the remanence of the "sample" which is reconstituted from all its specimens, as would be measured by a rock magnetometer designed to take large samples. Other approaches which are described in the literature, such as averaging remanent intensities of specimens to estimate the remanent intensity of sample or formation and combining specimen NRM directions as unit vectors (the palaeomagnetic procedure) to give a sample or formation NRM direction are invalid in the context of magnetic petrophysics (except in special cases).

Similarly, the sample susceptibility tensor is the unweighted sum of the specimen susceptibility tensors divided by their number. The resultant tensor is diagonalised to obtain major, intermediate and minor susceptibilities, which are then averaged to give the sample bulk susceptibility. These procedures yield values of magnetic properties pertaining to larger volumes of rock than to $10cm^3$ specimens, reducing the scatter of values associated with small scale inhogeneity.

Many of the samples collected from outcrops have NRM directions which are highly divergent from the characteristic direction for the area and some of these exhibit remarkably high Q values. These samples are asterisked in Tables 3 and 4. Such magnetisations are almost certainly lightning-induced. The remaining outcrop samples appear to have escaped significant IRM overprinting and their NRMs may be regarded as representative of oxidised BIF.

Examination of Tables 3 and 4 reveals several notable features:

(i) the properties of the Paraburdoo ore samples are remarkably uniform with bulk susceptibilites, which are distributed over a relatively small range ($30-200 \times 10^{-6}$), grouped about a mean value of 112×10^{-6} with standard error 12×10^{-6}. The NRM directions are well-grouped about the mean direction (NW with shallow negative

inclination). There is little evidence of streaking towards the present field direction due to VRM overprinting and palaeomagnetic cleaning reveals that the remanence is monocomponent. NRM intensities are also fairly consistent (mean ± SE: 73 ± 11 γ, neglecting two samples with divergent directions) and Koenigsberger ratios much greater than unity predominate. Given the consistent NRM direction, this implies that remanence overwhelmingly dominates induced magnetisation for the 4E orebody.

(ii) By contrast with the Paraburdoo ore samples, ore and mineralised BIF samples from Tom Price (TP03, 04, 08, 09) have much more variable properties and are significantly more magnetic overall. These properties reflect the presence of small but variable quantities of magnetite, whereas haematite is the only important magnetic mineral in the Paraburdoo ores. As discussed earlier the palaeomagnetic history of the Tom Price deposit is significantly more complex, resulting in considerable scatter in NRM directions. The generally Lower Koenigsberger ratios reflect both the multicomponent nature of the NRMs and the presence of magnetite as the major remanence carrier. In spite of the scatter, there is a predominance of directions in the NW up octant, broadly consistent with the characteristic direction of the Paraburdoo ores and fresh BIFs and with the majority of directions from the oxidised but unmineralised BIFs in and around the Tom Price mine.

The magnetic properties of all samples were sorted according to locality and lithology and then combined to calculate "formation" mean remanence vectors and susceptibility ellipsoids, using the procedure described above for calculating sample means. The induced, remanent and resultant magnetisations for the various lithologies (in their present orientations), together with the corresponding Koenigsberger ratios, are given in Table 5. N represents the number of specimens for which the original NRM could be estimated, following the removal of any IRM noise, and which could be confidently oriented. The calculated induced magnetisations reflect the intrinsic anisotropy of the rock unit, but

not self-demagnetisation (which is important for the BIFs).

The anisotropy parameters given in Table 6 are calculated from the listed apparent susceptibility ellipsoids, measured by the Digico anisotropy delineator, and corrected for self-demagnetisation of the specimen, assuming the specimen is homogeneous. If the rock fabric which produces the susceptibility anisotropy is of small scale, relative to the specimen size, then the apparent anisotropy corresponds to the intrinsic anisotropy of the bulk rock. This is the case for the ore specimens. The anisotropy of BIF, however, is a textural anisotropy arising from self-demagnetisation normal to the plane of layering of the highly magnetic bands. The scale of banding produces a sampling problem (this is a general feature of analytical studies on such inhomogeneous rocks as BIFs) and can also distort the apparent anisotropy. A specimen consisting of a single relatively homogeneous magnetic band will indicate the intrinsic anisotropy of that band, which is much less than the externally observed anisotropy due to that band. A specimen containing one (or a few) very thin magnetic bands within non-magnetic material, in effect simulates a BIF on a small scale. The standard correction for self-demagnetisation, assuming a homogeneous quasi-spherical specimen, then overestimates the externally observed anisotropy due to such bands. Because of these uncertainties an alternative approach to estimation of the anisotropy of the BIFs will be taken in the next section. This serves as a check on the tabulated measurements and as an aid to understanding.

Bearing in mind that the effective anisotropy of the BIFs is likely to be underestimated, because self-demagnetisation has been neglected, the true induced magnetisation vectors should be somewhat further deflected towards the bedding plane and their magnitudes should be modified, depending on the structure. Thus the resultant magnetisations and the Koenigsberger ratios cited for the fresh BIFs are only approximate, but are useful as semi-quantitative results.

From Table 5 it is apparent that the ores, with the exception of a zone of magnetic Marra Mamba ore from Paraburdoo, whilst they would be considered moderately magnetic in most environments, are much more

weakly magnetised than fresh BIF. The magnetic signature of mineralised and oxidised BIF should be therefore relatively flat and generally low with respect to surrounding BIF units. The magnetisation of fresh BIF units at Paraburdoo is typically about 6000γ, whilst the Dales Gorge member at Tom Price is more strongly magnetised, reflecting the higher magnetite content which is evident in the data of Ewers and Morris (1981). The resultant magnetisation is, broadly speaking, of normal polarity, but is significantly oblique to the present field due to the prominent, even dominant, contribution of the remanence (NW with low negative inclination). Quantitative interpretation of BIF structure clearly requires consideration of the characteristic remanence of the BIFs, which was shown in the palaeomagnetism section to be pre-folding, at least at Paraburdoo and Wittenoom.

In summary, the magnetisation of fresh BIF units reflects contributions of comparable magnitude from induced and remanent magnetisations, the induced magnetisation reflecting strong anisotropy. The remanent intensity is typically 4000 ± 1500 γ and the best estimate of its direction with respect to bedding is from Table 1, dec = 314°, inc = -5°. For tilted units the remanence direction can be calculated using the method of Clark (1983), which is also given in Appendix IV.

3.3 Magnetic anisotropy of BIF

We model a BIF unit as a succession of infinite, parallel, homogeneous, magnetic layers, each of uniform thickness, sandwiched between non-magnetic layers. The model does not require individual layers to be evenly spaced or to have the same thickness. We define the following parameters:

f	=	volume fraction of magnetite within the magnetic layers
k_i	=	intrinsic susceptibility of the magnetite grains
N	=	average demagnetising factor for an isolated magnetite grain
k	=	the intrinsic susceptibility of the magnetic layers
f_L	=	the volume fraction of the BIF comprised of magnetic layers

$k_=$ = the externally observed susceptibility of the BIF parallel to the layering

$k_\perp$ = the externally observed susceptibility of the BIF normal to the layering

A = anisotropy ratio = $k_=/k_\perp$

The effective demagnetising factor of each magnetite grain, taking grain interactions into account via the Lorentz field, is approximately N(1-f). The intrinsic susceptibility of the layers is then given by the Puzicha formula:

$$k = fk_i/[1 + N(1-f)k_i] \quad (1)$$

Because uniformly magnetised infinite sheets generate no external anomaly there is no interaction between the magnetic layers. The demagnetising factors parallel to and perpendicular to the layers are 0 and 4π respectively.

$$k_= = f_L k \quad (2)$$

$$k_\perp = f_L k/(1+4\pi k) \quad (3)$$

$$A = 1+4\pi k \quad (4)$$

Note that the effect of self-demagnetisation of the whole BIF, assumed to be a flat slab of great lateral extent relative to its thickness, is included in the calculated anisotropy.

$$\bar{k} = (2/3)k_= + (1/3)k_\perp \quad (5)$$

The magnetic layers correspond to magnetite and chert-matrix mesobands within BIF macrobands. Magnetite grain size ranges from 50-500 μm with a typical value of 200 μm (Trendall and Blockley, 1970, p.123). Dilute dispersions ($f \to 0$) of such large multidomain grains were found by Parry (1980) to be characterised by an observed susceptibility of 0.31 G/Oe (normalised to 100% magnetite) with an effective demagnetising factor of 2.9 Oe/G. Substituting k/f = 0.31, N = 2.9 into eqn (1) and solving for k_i gives k_i = 3.1 G/Oe. as $f \to 0$

The volume fraction of magnetite in the magnetite mesobands ranges from 50% to 95% (Trendall and Blockley, 1970, p. 108), with 80%

representing a typical value. Such mesobands constitute 13.3% of the BIF macrobands of the type-section Dales Gorge member (Trendall and Blockley, 1970; Table 4). The contribution of magnetite mesobands to the susceptibility of the Dales Gorge member can therefore be estimated by substituting k_i=3.1, f=0.8, N=2.9, f_L = 0.13 into eqns (1)-(5).

$$k_{=} = 0.115,\ k_{\perp} = 0.0095,\ \bar{k} = 0.080,\ A = 12.1 \qquad (6)$$

A significant proportion of the magnetic content of the BIFs occurs within chert-matrix mesobands, which typically contain 30-50% magnetite and which comprise 21.1% of the BIF macrobands in the Dales gorge type-section (Trendall and Blockley, 1970; pp. 47, 50). Taking k_i=3.1, f=0.4, n=2.9, f_L=0.21 we obtain for the chert-matrix mesobands:

$$k_{=} = 0.041,\ k_{\perp} = 0.012,\ \bar{k} = 0.031,\ A = 3.4 \qquad (7)$$

Combining the contributions in eqns (6) and (7) the estimated total susceptibility of BIF macrobands within the Dales Gorge member, ignoring the minor magnetite content of chert mesobands, is:
$k_{=} = 0.156,\ k_{\perp} = 0.0213,\ \bar{k} = 0.111,\ A = 7.3$

The BIF macrobands typically constitute about 80% of the Dales Gorge member, using data from Ewers and Morris (1981). Ignoring the minor magnetite content of the S macrobands, the effective susceptibility for the whole Dales Gorge member is estimated as:

$$k_{=} = 0.125,\ k_{\perp} = 0.017,\ \bar{k} = 0.089,\ A = 7.3 \qquad (8)$$

The values in eqn (8) represent estimated susceptibilities applicable to aeromagnetic surveys, for which the sensor is sufficiently distant that the internal structure (i.e. the individual macrobands) of the Dales Gorge member can be ignored and the whole unit can therefore be modelled as a homogeneous anisotropic body.

Some variation in properties from locality to locality is to be expected due to the regional variations in magnetite content found by Ewers and Morris (1981). Calculating volume percentages from the

published weight % magnetite and bulk densities gives 10.2%, 20.2%, 20.6% for the BIF macrobands at Paraburdoo, Wittenoom and Tom Price respectively. The above assumptions regarding magnetite contents and thicknesses of magnetite mesobands and chert-matrix mesobands yield an estimate of 18.8% magnetite by volume at Wittenoom, in good agreement with the measured magnetite content. This lends support to the above calculations.

At Tom Price, which is thought to represent a higher grade of metamorphism, the S macrobands may be appreciably magnetic, judging from a calculated 11% magnetite by volume for S5. Magnetic S macrobands will enhance the overall susceptibilities of the Dales Gorge member, but reduce the anisotropy.

By assuming that the corresponding mesoband types at the three localities are of equal thickness, at least on average, and by using the measured magnetite contents of the BIF macrobands, it is possible to repeat the analysis, making various assumptions about the distribution of magnetite between the mesobands. Two sets of assumptions, representing what are thought to be the extreme possibilities, are considered at each locality. The results are given in Table 7. Case I at Wittenoon and Tom Price assumes a magnetite content of 80 volume % for the magnetite mesobands, with the remaining magnetite on the BIF macrobands being allocated to chert-matrix mesobands. A further assumption is made that the BIF macrobands are of equal total thickness at the three localities (this is known to be approximately true for Paraburdoo and Wittenoon) and that the variations in stratigraphic thickness of the Dales Gorge member therefore reflect differences in thickness of the shale macrobands. The thicknesses are estimated from the isopach map for the DGM in Trendall (1983). Case II assumes lower magnetite contents for magnetite and chert-matrix mesobands (60% and ~ 40% respectively), allocating 6% magnetite to the chert and other weakly magnetic mesobands.

At Paraburdoo the magnetite content is lower than at the other two localities, reflecting a much greater abundance of haematite. Because of the uncertainties regarding the distribution of magnetite between the

two types of mesoband, two cases are considered, representing the possible extremes. Case I assumes all magnetite is within magnetite mesobands, which, by assumption, form 13.3% of the BIF macrobands (as at Wittenoom) or 13.3% x 0.84 = 11.2% of the DGM at Paraburdoo (where shale macrobands form 16% of the total thickness). Case II assumes that the increased proportion of haematite at Paraburdoo is evenly partitioned between the magnetite and chert-matrix mesobands and that the magnetite level within magnetite mesobands is reduced to the minimum compatible with the definition, 50%. The magnetite content of the chert-matrix mesobands is then required to be 50%x0.45/0.8 = 28%. To account for the lower measured magnetite content of the BIF macrobands a large proportion of the lateral equivalents at Paraburdoo of magnetite mesobands at Wittenoom must be chert-matrix.

It is evident from Table 7 that the properties of the DGM are very sensitive to the distribution of magnetite as well as to the total magnetite content. For Paraburdoo case II the calculated bulk susceptibility is less than half the value for case I and the anisotropy ratio is much lower, 2.6, compared to 10.1 for case I. Case II seems to be based on more realistic assumptions and conforms more closely to the results in Table 6.

The estimated susceptibility parameters for Wittenoom in Table 7 are based on the most reliable information and suggest that the type-section DGM has a high susceptibility (k=0.06-0.09 G/Oe) with high anisotropy (A=3-7). Again, the calculated parameters are rather sensitive to the assumed distribution of magnetite. Measurements of susceptibility anisotropy of seven specimens from the type-section DGM give $k_{=} = 0.066$, $k'_{\perp} = 0.026$, $A' = 2.6$, corresponding to an effective anisotropy A=3.4. These results strongly favour the assumptions of Case II over Case I, suggesting that the analogous assumptions are most likely to produce realistic estimates for the susceptibility parameters at Tom Price. The low intrinsic anisotropy of the DGM samples from Tom Price supports this conclusion. The very high bulk susceptibility of the DDH 93/80 samples is not representative of the member on the whole, because samples were taken from the most magnetic sections of the core.

Although the results given in Table 7 are only suggestive, not definitive, it seems that regardless of how the assumptions are juggled the anisotropy of the type-section DGM must be quite high (A>3). This has important implications for magnetic interpretation and for palaeomagnetism.

R.C. Morris (pers. comm.) points out that the mesobands are not really isotropic, as the magnetite tends to occur as thin rafts or plates. Unless the rafts are strongly interacting this will give rise to an even higher anisotropy. If all the magnetite in the BIF were concentrated into thin continuous layers the anisotropy would approach the theoretical maximum $1+4\pi k_1 \simeq 40$. However the geometry of the magnetite distribution and the anisotropy measurements themselves suggest that the mesobands are not intrinsically highly anisotropic. To apply the theory presented in this section with confidence more information on magnetite concentrations and distribution within and between mesobands is needed.

As an example of the importance of anisotropy to magnetic interpretation consider the induced magnetisation of a flat-lying BIF unit, as at Wittenoom. The inclination of the Earth's field is -56° but the induced magnetisation is deflected towards the bedding plane through 30° (i.e. I = -26°) for A = 3 and through 44° (I = -12°) for A = 7. By ignoring anisotropy interpreted dips will be in error by similar amounts (neglecting additional complications due to remanence).

Having examined the Dales Gorge member in detail it is possible to discuss the properties of the other BIF units, at least qualitatively. Much less information is available concerning the magnetite distribution of these units, but some measurements of susceptibility have been made, either in this study, by Chamalaun and Dempsey (1978) or by Embleton et al. (1979).

Macrobanding is absent from the Joffre member and ~50% of the total thickness consists of chert-matrix mesobands which contain rare, thin, magnetite mesobands (Trendall and Blockley, 1970). Although the total iron content (~ 28 wt%) is similar for the Dales Gorge and Joffre

members the Fe^{3+}/Fe^{2+} ratio is lower for the Joffre (~1.0 as opposed to ~1.5 for the DGM and 2.0 for magnetite), suggesting that the total magnetite content is somewhat lower in the Joffre member. These facts suggest that the Joffre member should have somewhat lower bulk susceptibility and anisotropy then the DGM. This expectation is borne out by the measurements on drill-core samples reported in Table 6. Measurements on seven specimens from the Joffre member at Wittenoom Gorge (DH 47A), however, give $k_{=} = 0.082$, $k'_{\perp} = 0.034$, $A' = 2.4$ (corresponding to an effective anisotropy $A = 3.4$) which gives a slightly higher susceptibility than for the DGM specimens from hole 51. The measured anisotropy of the two formations is comparable. Surface samples of the Joffre member were found by Chamalaun and Dempsey (1978) to have slightly lower susceptibility, on average, than DGM samples. At least some specimens had high anisotropies. Taken together, the evidence suggests that the typical bulk susceptibilities and anisotropies of the Dales Gorge and Joffre members are similar.

Trendall and Blockley (1970) state that magnetite is rare in the Weeli Wolli formation; however no fresh material was available at that time. Our measurements indicate that fresh Weeli Wolli BIF at Paraburdoo is strongly magnetic. Chamalaun and Dempsey (1978) found relatively fresh exposures of WW BIF to have somewhat higher susceptibility than the Brockman Iron Formation. The mean susceptibility normal to bedding was 0.066 G/Oe and the mode was 0.05 G/Oe.

Trendall and Blockley (1970) describe the Boolgeda formation as intensely magnetic. Analyses show the total iron content of the Boolgeda formation to be similar to that of the Brockman IF but that the Fe^{3+}/Fe^{2+} ratio is much higher (~3.4), suggesting an increased proportion of haematite. Embleton et al. (1974) found that the magnetic properties were somewhat variable but overall were similar to those of the Brockman IF. Chamalaun and Dempsey (1978) presented a histogram of perpendicular susceptibilities of Boolgeda surface samples which showed a very broad distribution, with a mean value of 0.012 G/Oe. Some of the observed variation is certainly intrinsic inhomogeneity, but many of the lower values probably reflect weathering. Specimens of Boolgeda IF are also highly anisotropic (A'~2.6).

The Marra Mamba formation resembles the Joffre member in that magnetite mesobands are absent. The chert-matrix mesobands contain magnetite laminae (Trendall and Blockley, 1970). Marra Mamba BIF seems particularly prone to weathering, which probably biases magnetic property measurements on surface samples. Chamalaun and Dempsey (1978) found a broad distribution of perpendicular susceptibilities with a mean of 0.021 G/Oe.

The earlier studies showed that NRMs of surface samples of the various BIF units were scattered but showed a tendency to fall in the NW up octant. AF cleaning emphasised the NW up component which appears to be ubiquitous in the Hamersley basis and it seems reasonable to conclude that the representative in situ NRM of the BIFs is similar in direction to that of the Brockman and Weeli Wolli formations.

Overall the magnetic properties of all the BIFs seem to be fairly similar and all can be expected to contribute analogously to magnetic anomalies.

The susceptibility parallel to bedding probably lies in the range 0.05 - 0.1 G/Oe in most localities, with an intrinsic anisotropy of 2-4. Remanence appears to contribute significantly to the total magnetisation with Q values typically 1-2.

4. Magsat Anomaly over the Hamersley Group

At satellite heights the Hamersley Basin can be adequately represented by a thin horizontal slab. Using the data of Trendall and Blockley (1970) the slab is assigned a thickness of 1 km, representing the average total thickness of BIF units in the basin, and horizontal dimensions of 500 km x 120 km, the long axis striking 260°. This rectangle corresponds reasonably well to the present distribution of the Hamersley group, which has a total outcrop area of 60,000 km^2.

If the model is assigned plausible values for susceptibility and NRM an anomaly of several gammas is predicted at a height of 400 km. In particular, taking $K_{\perp}$ = 0.03 G/Oe, A = 3, and assuming a pre-folding or post-folding remanence with Q=1 the theoretical anomaly is of dipolar

form, with the high to the north, and has a total amplitude of ~6γ. the amplitude corresponds well to that of the observed anomaly. The anomaly shape differs from that shown in the MAGSAT anomaly map of Australia (Mayhew et al., 1980), which shows a fairly symmetric high over the Hamersley Basin. However the base level and trend are highly uncertain for these MAGSAT anomalies, due to incomplete removal of external fields (Johnson, 1985) and the "observed" anomaly shape may be distorted.

Even reducing the magnetisation of the model to the minimum plausible level suggests that the response due to the BIFs must exceed 3γ at 400km. Thus we conclude that at least part, and probably most, of the MAGSAT anomaly associated with the Hamersley province arises from the BIFs.

It is unusual for a shallow crustal feature to be clearly reflected in MAGSAT data. In this case the intense magnetisation and relatively large volume (~ 60,000 km^3) of BIFs is responsible.

Recognition of this MAGSAT feature as of superficial origin, many have important ramifications for interpretation of crustal magnetisation distribution (inferred by inversion of the MAGSAT anomalies) in terms of crustal thickness, tectonic province and heat flow.

REFERENCES

Chamalaun, F.H. and Dempsey, C.E., 1978. A survey of the magnetic properties of the banded iron formations, Hamersley Province, W.A., Earth Sciences, Flinders University Publication No. 78/4, 51 pp.

Clark, D.A., 1983. Comments on magnetic petrophysics. Bull. Aust. Soc. Explor. Geophys., 14, 49-62.

Embleton, B.J.J., 1978. The palaeomagnetism of 2400 m.y. old rocks from the Australian Pilbara craton and its relation to Archaean-Proterozoic tectonics, Precambrian Res. 6, 275-291.

Embleton, B.J.J., 1981. A review of the palaeomagnetism of Australia and Antarctica, in "Paleoreconstruction of the continents, Geodyn. Ser., Vol. 2, ed. M.W. McElhinny and D.A. Valencio, pp. 77-92, AGU, Washington, D.C.

Embleton, B.J.J., Robertson, W.A. and Schmidt, P.W., 1979. A survey of magnetic properties of some rocks from northwestern Australia. Invest. Rep. 129, CSIRO, Div. of Min. Phys., Sydney.

Emerson, D.W., Clark, D.A. and Saul, S.J., 1985. Magnetic exploration models incorporating remanence, demagnetization and anisotropy: HP41C handheld computer algorithms. Explor. Geophys., 16, 1-22.

Eskola, L. and Tervo, T., 1980. Solving the magnetostatic field problem (a case of high susceptibility) by means of the method of subsections. Geoexploration, 18, 79-95.

Ewers, W.E. and Morris, R.C., 1981. Studies of the Dales Gorge Member of the Brockman Iron Formation, Western Australia. Econ. Geol., 76, 1929-1953.

Fisher, R.A., 1953. Dispersion on a sphere. Proc. R. Soc. Lond., A217, 295-305.

Fuller, M. 1969. Magnetic orientation of borehole cores. Geophysics, 34: 772-774.

Grauch, V.J.S. and Campbell, D.L., 1984. Does draping aeromagnetic data reduce terrain-induced effects? Geophysics, 49, 75-80.

Henry, W.E., 1982. Palaeomagnetic methods for orientation of borehole cores, Horizon Cleveland Field, Ochiltree Country, Texas. AAPG Bull., 66, p. 244.

Hjelt, S.O. and Phokin, A.P., 1981. Interpretation of borehole magnetic data and some special problems of magnetometry. Dept. of Geophys., Univ. of Oulu, Finland, Rep. No. 1, 171 pp.

Kodama, K.P., 1984. Palaeomagnetism of granitic intrusives from the Precambrian basement under eastern Kansas: orienting drill cores using secondary magnetization components. Geophys. J.R. astr. Soc., 76, 273-287.

Lynton, E.D., 1938. Recent developments in laboratory orientation of cores by their magnetic polarity. Geophysics, 3, 122-129.

Mayhew, M.A., Johnson, B.D. and Langel, R.A., 1980. An equivalent source model of the satellite magnetic field over Australia. Earth Planet. Sci. Lett., 51, 189-198.

McFadden, P.L. and Jones, D.L., 1981. The fold test in palaeomagnetism. Geophys. J.R. astr. Soc., 67, 53-58.

Morris, R.C., 1980. A textural and mineralogical study of the relationship of iron ore to banded iron-formation in the Hamersley iron province of Western Australia. Econ. Geol., 75, 184-209.

Parry, L.G., 1980. Shape-related factors in the magnetization of immobilized magnetite particles. Phys. Earth Planet. Int., 22, 44-154.

Porath, H. and Chalalaun, F.H., 1968. Palaeomagnetism of Australian haematite ore bodies. II. Western Australia. Geophys. J.R. astr. Soc., 15, 253-264.

Ridley, B.H. and Brown, H.E., 1980. The transformer bridge and magnetic susceptibility measurement. Bull. Aust. Soc. Explor. Geophys., 11, 110-114.

Schmidt, P.W. and Clark, D.A., 1985. Presentation and analysis of palaeomagnetic data. Restric. Invest. Rep. 1602R, CSIRO Div. of Min. Physics. and Mineralogy, Sydney.

Schmidt, P.W. and Clark, D.A., 1986. Step-wise and continuous thermal demagnetization and theories of thermoremanence, Geophys. J.R. astr. Soc., 83, 731-751.

Schmidt, P.W. and Embleton, B.J.J., 1985. Pre-folding and overprint magnetic signatures in Precambrian (~2.9-2.7 Ga) igneous rocks from the Pilbara Craton and Hamersley Basin, N.W. Australia. J. Geophys. Res., 90, 2967-2984.

Trendall, A.F., 1983. The Hamersley Basin, in "Iron-formations: facts and problems", Developments in Precambrian Geology 6, eds. A.F. Trendall and R.C. Morris, Elsevier, Amsterdam, pp. 69-129.

Trendall, A.F. and Blockley, J.G., 1970. The iron associations of the Precambrian Hamersley Group, Western Australia, with special reference to the associated crocidolite. West. Aust. Geol. Survey Bull. 119.

Table 1 Summary of magnetisation directions after treatment

Unit	N	D_H^o	I_H^o	α_{95}^o	D_B^o	I_B^o	α_{95}^o
DDH42	9	294.3	-35.1	7.7	311.7	-2.4	7.7
DDH44	12	290.5	-42.2	8.7	315.7	-6.5	8.7
DDH42+44	21	292.2	-39.1	5.8	314.0	-4.7	5.8
DDH3+4	8	335.3	-16.9	36	334.0	24.0	36
DDH93	15	249.6	-5.1	22	257.4	-16.9	22
PB+	15	304.7	-23.0	8.3	316.0	-6.9	8.7
TP+	19	308.8	-9.3	11.2	300.2	-16.0	14.7

Abbreviations: N - number of samples used; D - declination; I - inclination, H - with respect to present horizontal, B - with respect to bedding (taking into account plunges), i.e. with respect to palaeohorizontal, α_{95} - half-angle of Fisher's (1953) cone of 95 percent confidence within which the true mean direction probably falls. + These results refer to surface samples.

Table 2. Summary of the paleomagnetic data for Australia for Precambrian time > 700 Myr

Region	Rock Unit	Fig. 1 mnemonic	Age Myr	Pole position Lat.N	Long.E	A_{95} (dp,dm)
Gawler craton	dykes, group GB	GB	1700±100	23°	266°	11°
	dykes, group BA	GA	1500±200	61°	231°	9°
	Gawler Range Volcanics	GR	1525±15	60°	230°	6°
	Iron Monarch, +ve group	IMP	1800-1500	15°	272°	12°
	Iron monarch, -ve group	IMn	1800-1500	64°	267°	9°
	Iron Prince	IP	1800-1500	39°	247°	10°
Mt. Isa Province	dykes, group IB	IB	<1700	53°	282°	11°
	Lunch Creek Gabbro	LC	~1500	63°	021°	9°
	Lake View dolerite	IA	1150	12°	304°	11°
Hall Creek Province	Hart dolerite	HD	1800±25	29°	046°	24°
Musgrave Block	Giles complex	GC	1250-1140	68°	343°	(23°, 29°)
Pine Creek Geosyncline	Edith River Volcanics	ERV	~1760	06°	014°	(15°, 24°)
Yilgarn craton	dykes, group YE	YE	2500±200	28°	180°	31°
	Ravensthorpe dykes	RD	2500±100	38	316°	25°
	Widgiemooltha dykes	WD	2420±30	09°	337°	8°
	dykes, group YA	YA	~2500or~1700	22°	314°	18°
	Koolyanobbing-Dowds Hill	KD	2750-220	43°	356°	9°
	Koolyanobbing-'A' deposit	KA	-	26°	092°	17°
	dykes, group YF	YF	~1700	25°	102°	14°
	dykes, group YD	YD	~1700	24°	226°	10°
	dykes, group YC	<1500		80°	003°	13°
	Morowa Lavas	ML	1390±140	43°	022°	15°
	dykes, group YB	YB	~750	20°	102°	28°
	Duffer Formation	DFH	~2600	19°	183°	15°
	" "	DFM	3452	44°	86°	7°
	" "	DFL	~3000	55°	132°	13°
	Hamersley BIF	PBA	~2500?	-41°	226°	(3°, 6°)
		WN	~2500?	-37°	219°	(5°, 9°)
	Paraburdoo ore (H)*	PBB		-30°	216°	(5°, 9°)
	(B)+	"		-46°	223°	(5°, 9°)
	Tom Price ore (H)*	TPB		-40°	217°	(6°, 11°)
	(B)+	"		-32°	211°	(8°, 15°)
Pilbara craton	Black Range dyke	BR	2329±89	32°	334°	9°
	Cajuput dyke	CD	~2400	46°	326°	22°
	Mt. Goldsworthy lode ore	MG3	3000-2000	31°	330°	13°
	Mt. Goldsworthy lode ore	MG1	<MG3	20°	084°	6°
	Mt. Goldsworthy crust ore	MG2	<MG1	22°	259°	19°
	Mt Tom Price	TP	~1800	22°	057°	12°
	Mt Newman	MN	~1800	17°	066°	10°

Myr = million years; Lat. = latitude; Long. = longitude; A_{95} = semi angle of the cone of 95% confidence (Fisher 1953) around the pole; dp,dm = the semi-axes of the elliptical error around the pole at a probability of 95%, dp in the colatitude direction and dm perpendicular to it.

* With respect to present horizontal (in situ)

+ With respect to ancient horizontal (after unfolding beds).

Table 3 Magnetic Properties of Paraburdoo Surface Samples

Sample	Exposure	Bulk susceptibility x 10^6	NRM	Q
PB01A	E	140	175; 314°,-17°	23.4
PB01B	E	110	100; 325°,-11°	16.5
PB01C	E	150	90; 303°,-20°	11.4
PB02A	E	120	50; 327°,-2°	7.8
PB02B	E	110	120; 320°, -39°	19.4
PB02C	E	150	140; 316°,-39°	17.3
PB03A	E	200	75; 288°,-37°	6.8
PB03B	E	130	45; 304°,+13°	6.2
PB03C	E	175	40; 292°, -38°	4.0
PB04A	E	55	50; 298°, -25°	16.3
PB04B	E	80	50; 300°, -31°	11.4
PB04C	E	50	4; 311°, -29°	1.5
PB05A	O	30	2; 310°, -62°	1.3
PB05B	O	2320	11; 224°, -20°	0.1
PB05D	O	30	2; 343°, -62°	1.1
PB06A	O	155	17; 334°,-52°	2.0
PB06B*	O	195	110; 64°, +38°	10.6
PB06C*	O	910	1520; 317°, +46°	30.4
PB07A	E	175	90; 303°, -27°	9.6
PB07B	E	30	25; 291°, -20°	17.3
PB07C	E	80	75; 309°, -31°	17.2
PB08A	E	55	5; 214°, -61°	1.6
PB08B	E	-	55; 37°, +50°	-
PB08C	E	105	45; 332°, -35°	7.6
PB09A*	O	65	183; 117°, -13°	54.0
PB09B	O	140	50; 42°, +49°	6.5
PB09C*	O	2800	10,640; 4°, +9°	70.6
PB09D	O	95	80; 334°, 1°	16.0

* Affected by lightning

Bulk susceptibility k is mean of major, intermediate and minor susceptbilities for anisotropic rocks. Cgs (emu) units are used here. NRMs are expressed in the form (J; D, I) where J is the intensity of magnetisation in gammas (1γ=10μG), D is the declination (measured positive clockwise from TN) and I is the inclination (positive downward).

Q is the Koenigsberger ratio and is equal to remanent intensity/induced intensity. The induced magnetisation is given by $\tilde{J}_{IND} = K\tilde{F}$, where K is the susceptibility tensor and F is the Earth's field, with magnitude 53,800γ, declination 1° and inclination -56°.

E = excavated, O = (natural) outcrop.

Table 4 Magnetic Properties of Tom Price Surface Samples

Sample	Bulk susceptibility x 10^6	NRM	Q
TP01A	320	17; 338°,-4°	0.97
TP01B	460	21; 351°, -35.5°	0.85
TP01C	545	17; 309°, -2°	0.58
TP02A	9200	245; 352°, 2°	0.57
TP02B	4000	1330; 328°, -16°	6.2
TP02C	11,380	310; 288°, -12°	0.60
TP03A	990	85; 286°, -30°	1.6
TP03B	890	110; 278°, -20°	2.3
TP03C	-	5; 64°, 7°	-
TP04A	65	5; 155°, -27°	1.4
TP04B	460	20; 102°, -5°	0.71
TP04C	-	30; 275°, +25°	-
TP05A	14,600	1100; 322°, -10°	1.5
TP05B	1190	9; 188°, -58°	0.17
TP05C	3770	420; 323°, -1°	2.2
TP06B	110	11; 345°, -64°	1.9
TP06C	1425	20; 71, -20	0.27
TP07A	95	14; 344°, -65°	2.6
TP07B	50	25; 327°, -10°	8.8
TP07C	100	30; 313°, -16°	5.7
TP08A	150	65; 354°, -13°	8.0
TP08B	160	14; 108°, -7°	1.7
TP08C	180	15; 152°, +2°	1.6
TP09A	820	140; 298°, -36°	3.2
TP09B	2660	165; 300°, -28°	1.3
TP09C	4100	220; 302°, -44°	1.1
TP10A*	7230	4200; 29°, -12°	11.2
TP10B*	11,200	2150; 10°, 39°	3.8
TP10C	75	25; 311°, -24°	5.8
TP11A	4660	360; 288°, -16°	1.7
TP11B*	12400	795; 135°, -4°	1.4
TP11C	60	0.3; 332°, -78°	0.10
TP12A	320	1320; 257°, -49°	76.6
TP12B	1060	1080; 289°, -11°	20.7
TP12C*	5750	1820; 65°, -7°	6.5
TP13A*	150	5100; 35°, 8°	632
TP13B*	530	2860; 250°, -1°	100
TP13C*	90	12,260; 235°, -12°	2530
TP14A	500	1505; 330°, -9°	56
TP14B*	205	6730; 95°, 10°616	610
TP14C	725	930; 285°, -32°	23.4

Symbols as for Table 2. TP01 -06, 08-09 in mine; TP07, TP10-14 natural outcrop.

Table 5 Mean Magnetisations

Lithology	Exposure	N	J_{IND}	J_{NRM}	J_{RES}	Q
Tom Price ore and oxidised and oxidised BIF (sites TP01-09)	E*	24	120; 3°, -52°	170; 323°, -16°	261; 335°, -32°	1.4
Unmineralised, weathered BIF (sites TP10-14)	O	7	50; 356°, -55°	650; 295°, -26°	680; 298°, -29°	12.7
Paraburdoo ore and mineralised BIF (PB01-04, 07-08)	E	17	6; 1°, -56°	65; 310°, -26°	70; 313°, -29°	10.8
Marra Mamba oxidised BIF (PB05-06)	O	4	36; 1°, -53°	6; 283°, -57°	40; 353°, -56°	0.17
Tom Price ore and mineralised BIF (No 93/80)	D	9	38; 1°, -56°	95; 294°, -8°	114; 305°, -23°	2.5
Fresh Dales Gorge BIF (ND93/80, Tom Price)	D	4	12,900; 357°, -54°	6450; 283°, -17°	16,500; 324°, -48°	0.50
Shale (93/240.5m)	D	1	44; 3°, -55°	315; 266°, +1°	314; 270°, -6°	7.2
Fresh Dales Gorge BIF (DDH 42, Paraburdoo)	D	13	3100; 1.5°, -50°	2420; 294°, -20°	4790; 325°, -42°	0.78
Fresh Joffre BIF (DDH 44, Paraburdoo)	D	6	2330; 356°, -52°	3620; 283.5°, -26°	5210; 304°, -41°	1.6
Fresh Weeli Wolli BIF (DDH 44, Paraburdoo)	D	4	2150; 2°, -47°	5730; 306°, -38°	7480; 319°, -43°	2.7
Dolerite (DDH 44, Paraburdoo)	D	1	5; 1°, -56°	0.2; 300°, -47°	5; 359°, -56°	0.04
Marra Mamba ore (DDH 3, Paraburdoo)	D	7	135; 1°, -56°	31; 270°, -30°	38; 286°, -44°	2.3
Magnetic MM ore (DDH4, Paraburdoo)	D	4	290; 2°, -55°	2870; 348°, +7°	3010; 349°, +2°	9.9

* Except for TP 07 (natural outcrop in deep erosion gully)
E = excavated O = (natural) outcrop D = drill-core N = number of samples
J_{IND} = induced magnetisation vector J_{NRM} = remanent magnetisation vector J_{RES} = resultant magnetisation vector
$J_{IND} = KF$, where K = susceptibility tensor, F = Earth's field vector = (53800γ; 1°, -56°)
All magnetisations are given in form (J; D,I), where J is intensity in gammas (10μG = 1γ), D is declination, I is inclination
$J_{RES} = J_{IND} + J_{NRM}$
Q = Koenigsberger ratio = J_{NRM}/J_{IND}

Table 6 Mean Susceptibility Ellipsoids

Lithology	Exposure	N	Susceptibility ellipsoid	A'	L	F	P
Tom Price ore and mineralised BIF (TP01-09)	E	24	2610; 298°, +13°; 2500; 29°, +4° 2110; 38°, +76°	1.24	1.04	1.18	0.88
Unmineralised, weathered BIF (TP10-14)	O	15	3210; 321°, +19° 3070; 56°, +13° 2700; 178°, +66°	1.19	1.05	1.14	0.92
Paraburdoo ore and mineralised BIF (PB01-04,07-08)	E	17	k = 112	Isotropic			
Marra Mamba oxidised BIF (PB05, 06)	O	6	641; 116°, +20° 633; 221°, +35° 544; 2.5°, +48°	1.18	1.01	1.16	0.87
Tom Price ore and mineralised BIF (ND93/80)	D	9	k = 710	A = 1.03			
Fresh Dales Gorge BIF (ND 93/80, Tom Price)	D	4	243,600; 158°, +44° 212,600; 251°, + 2.5° 185,300; 343°, +46°	1.31	1.15	1.15	1.00
Shale 93/240.5m)	D	1	840; 57°, +29° 800; 309°, +29° 770; 183°, +46°	1.09	1.05	1.04	1.01
Fresh Dales Gorge BIF (DDH 42, Paraburdoo)	D	13	59,260; 236°, +29° 58,470; 127°, +30° 27,930; 001°, +46°	2.12	1.01	2.09	0.48
Fresh Joffre BIF (DDH 44, Paraburdoo)	D	6	49,670; 105°, +15° 43,090; 207°, +39° 29,440; 358°, +47°	1.69	1.15	1.46	0.79
Fresh Weeli Wolli BIF (DDH 44, Paraburdoo)	D	4	43,460; 226°, +18° 41,700; 129°, +21° 27,080; 353°, +62°	1.60	1.04	1.54	0.68
Dolerite (DDH44/Paraburdoo)	D	1	k = 93	Isotropic			
Marra Mamba ore (DDH3, Paraburdoo)	D	7	k = 249	A=1.04	-	-	-
Magnetic MM ore (DDH 4, Paraburdoo)	D	4	5560; 249°, +15° 5380; 146°, +40° 4580; 355°, +47°	1.21	1.03	1.17	0.88

E = excavated O = (natural) outcrop D = drill-core
N = number of specimens included in calculation
Susceptibility ellipsoids are given as k_1 (μG/Oe); D_1, I_1 [major axis]
k_2 (μG/Oe); D_2, I_2 [intermediate axis]
k_3 (μG/Oe); D_3, I_3 [minor axis]

A' = intrinsic anisotropy = k_1/k_3; L = magnetic lineation = k_1/k_2; F = magnetic foliation = k_2/k_3;
P = prolateness = L/F (P<1 indicates predominantly oblate [flattened] ellipsoid)

Table 7 Estimated susceptibilities for the Dales Gorge Member

	Paraburdoo		Wittenoom		Tom Price	
	Case I	Case II	Case I	Case II	Case I	Case II
BIF macrobands						
f (magnetite mesobands)	0.77	0.5	0.80	0.60	0.80	0.60
f (chert-matrix mesobands)	0.00	0.28	0.45	0.40	0.47	0.41
f ("chert" mesobands)	0.00	0.00	0.00	0.06	0.00	0.06
f_L (magnetite mesobands)	0.112*	0.022*	0.100		0.093*	
f_L (magnetite mesobands)	0.177*	0.267*	0.158		0.148*	
f_L ("chert" mesobands)	0.551*		0.492		0.459*	
f (BIF macrobands)	0.102		0.202		0.206	
Shale macrobands						
f	0.012		0.013		0.11	
f_L	0.16		0.25		0.30*	
Total thickness (m)	125		140		150	
Susceptibility parameters						
$k_=$ (G/Oe)	0.0878	0.0378	0.127	0.0815	0.131	0.0879
$k_\perp$ (G/Oe)	0.0087	0.0145	0.0177	0.0241	0.0234	0.0296
$\bar{k}$ (G/Oe)	0.0614	0.0301	0.0904	0.0623	0.0953	0.0684
A	10.1	2.6	7.2	3.4	5.6	3.0
A'	9.0	2.1	5.6	2.4	4.0	1.9

"chert" includes chert and miscellaneous weakly magnetic mesobands (carbonate, riebeckite etc.)

f_L = fraction of total stratigraphic thickness of DGM consisting of the designated lithology

$k_=$, $k_\perp$, $\bar{k}$ = externally observed or effective susceptibilities (parallel to layering, perpendicular to layering, bulk, respectively)

A = effective anisotropy (including self-demagnetisation of laterally extensive unit) = $k_=/k_\perp$

A' = intrinsic anisotropy of DGM (cf measured values in Table 5) = $A(1-4\pi k_\perp)$

* assumed value, not measured.

Fig. 1 Stereographic projections of natural remanent magnetisations of partially oriented drill core samples, measured with respect to their apparent down dip direction. the +X direction is aligned with the apparent down dip direction for each core piece, but in general this will not coincide with the true down dip direction for non-vertical drill holes. At localities sampled for this study, regional bedding attitude dipped southerly (to ~ 180°) therefore an approximate absolute orientation (with respect to geographical coordinates) can be reckoned by simply adding 180° to the declinations plotted.

a) Directions from Paraburdoo DDH 42 and DDH 44,

b) from Paraburdoo DDH 3 and DDH 4, and from Tom Price DDH ND93/80.

All open symbols refer to the upper hemisphere, while closed symbols refer to the lower (or obscured) hemisphere.

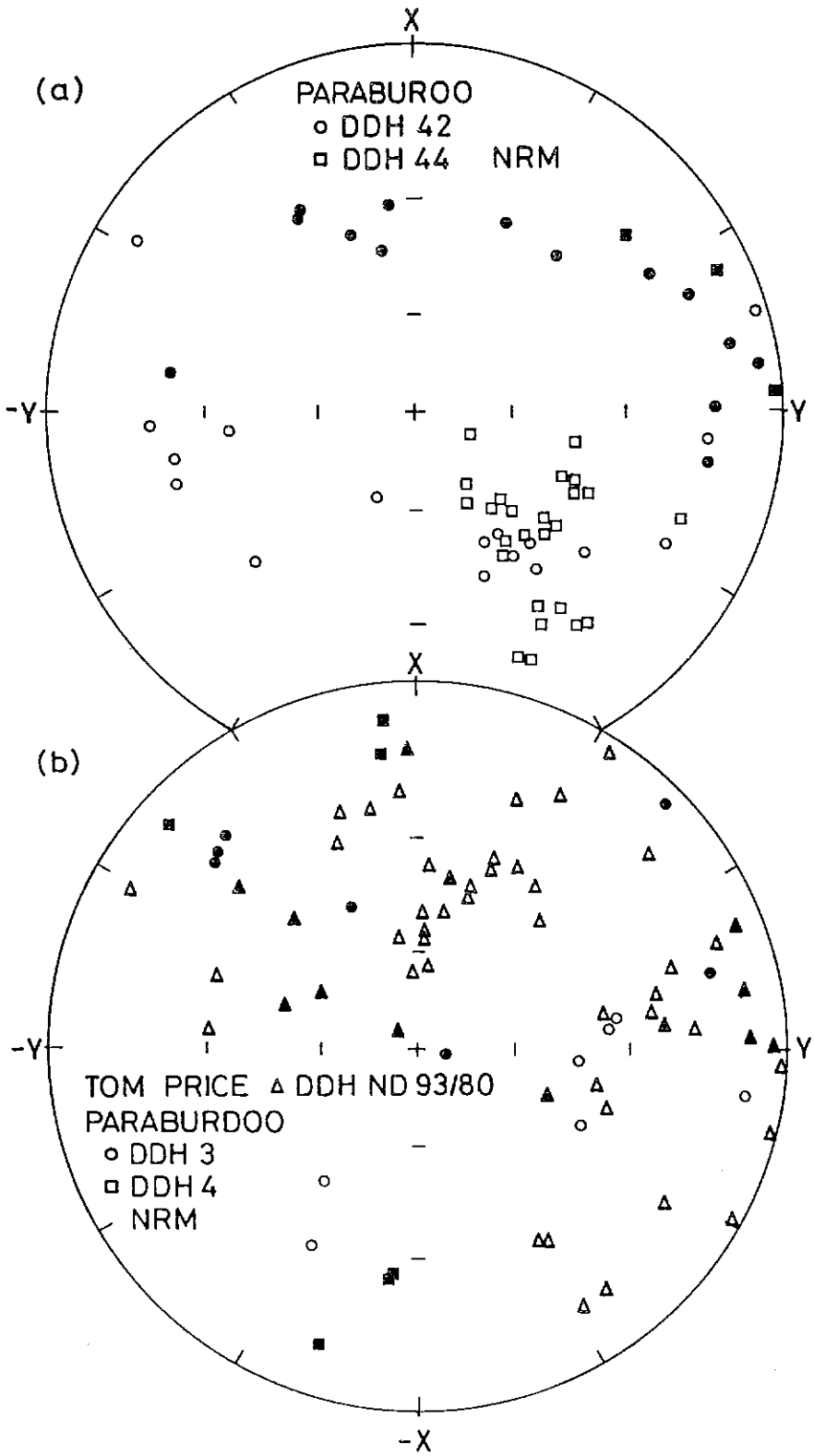
(a)
PARABUROO
o DDH 42
□ DDH 44 NRM
X
-Y
Y
(b)
TOM PRICE △ DDH ND 93/80
PARABURDOO
o DDH 3
□ DDH 4
NRM
-X

Fig. 2. Stereographic projections of magnetisation directions (plotted as on Fig. 1) showing changes in direction of some selected specimens after alternating field (AF) demagnetisation. The groups of three directions refer to each particular specimen's magnetisation when first measured (NRM), and after 50 Oe and 100 Oe peak AF demagnetisation.

a) In particular, magnetic directions from DDH 42 specimens converge on one octant, while many of those from DDH 93 diverge or change little.

b) AF demagnetisation has little effect on directions of magnetisation in DDH 3 and DDH 4. All symbols as for Fig. 1.

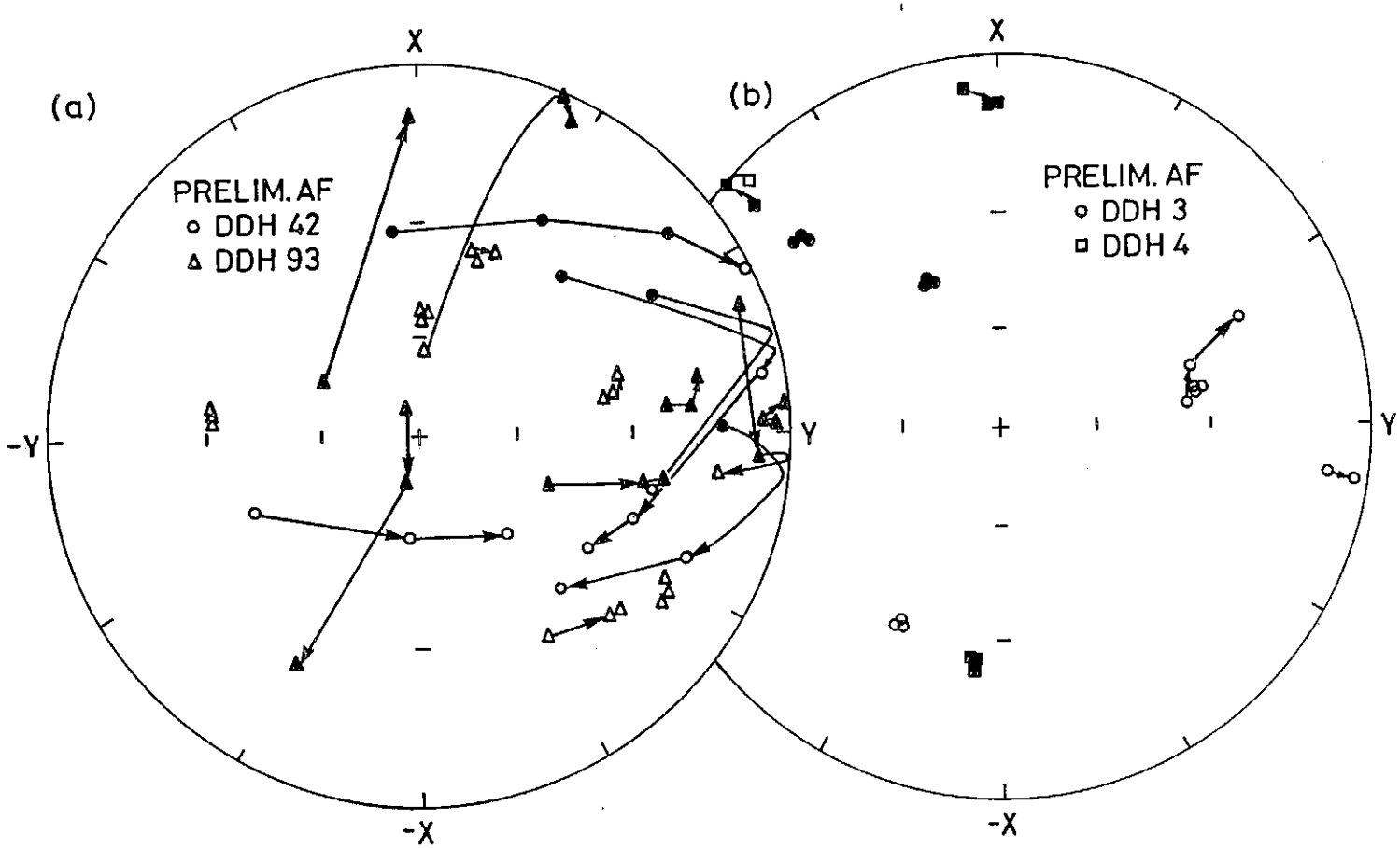
(a)
PRELIM. AF
DDH 42
DDH 93
X
-Y
Y
-X
(b)
PRELIM. AF
DDH 3
DDH 4
X
Y
-X

Fig. 3. Orthogonal projections of magnetisation vectors (with respect to apparent down dip direction, +X direction) after various demagnetisation steps, closed dots represent the projection of the vectors onto the horizontal (X-Y) plane, while the open dots represent projections onto the vertical (either Y-Z or X-Z) plane. This standard procedure of displaying palaeomagnetic data gives a full appreciation of both changes in direction and changes in intensity during the demagnetisation process, and enables any complex or multiple components of magnetisation to be visualised (Schmidt and Clark, 1985). Units are μG.

a) AF demagnetisation of specimen 44/49.8B (oxidised Weeli Wolli BIF) has little effect after the first (50 Oe) step.

b) Thermal demagnetisation of specimen 44/49.8A (duplicate of above specimen) has little effect on intensity until the Curie temperature (685°C) is exceeded when the intensity dramatically falls to zero. The direction also remains constant.

c) Thermal demagnetisation of riebekite specimen 42/207.0B following a single AF demagnetisation step of 50 Oe. Although the inclination remains fairly constant, the declination swings around from the (-X, -Y) quadrant, to the (-X,+Y) quadrant while the intensity decays steadily to the origin.

d) AF demagnetisation (50 Oe - 400 Oe) of a dolerite specimen 44/174.8C. Although intensity is weak (~1μG), direction remains constant after a slight change between NRM and 50 Oe. It is significant that the dolerite is magnetised in a direction similar to the BIF.

e) AF demagnetisation of specimen 42/207.0C (duplicate of 207.0B above) reveals a dramatic change of direction and intensity after 50 Oe. Direction swings from (-Y,-X) quadrant to the (-X,Y) quadrant as observed for 42/207.0B during thermal demagnetisation.

f) Expansion of e) demonstrating the consistency of direction at higher AF demagnetisation to 400 Oe.

Approximate geographic orientations for all these directions can be deduced by aligning the +X direction of each diagram with the regional down dip direction for this area (i.e. south). In effect this is adding 180° to the declinations, yielding directions that are NW and up.

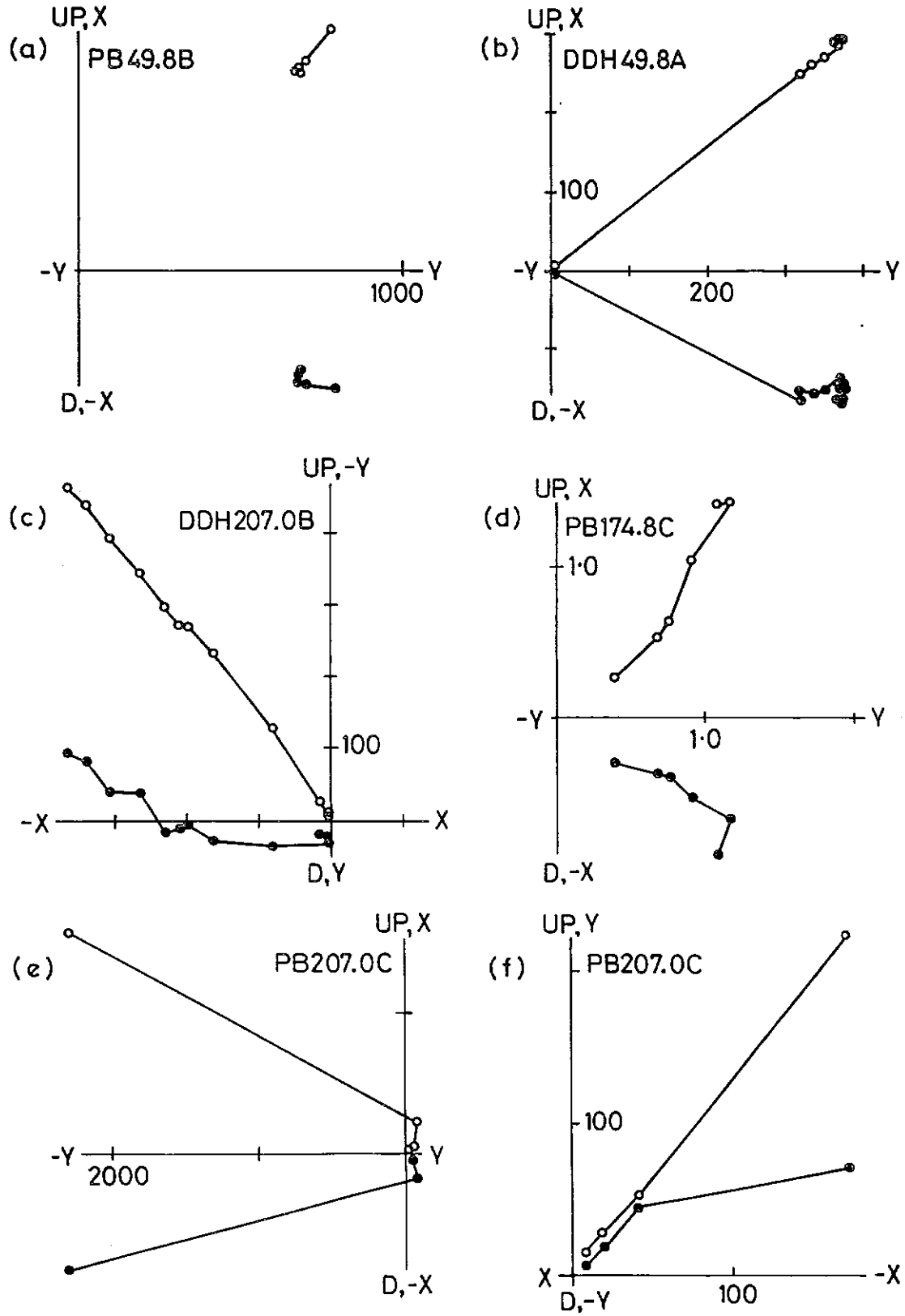
(a)
UP, X
PB 49.8B
-Y
Y
1000
D, -X
(b)
UP, X
DDH 49.8A
100
-Y
Y
200
D, -X
(c)
UP, -Y
DDH 207.0B
100
-X
X
D, Y
(d)
UP, X
PB 174.8C
1·0
-Y
Y
1·0
D, -X
(e)
UP, X
PB 207.0C
-Y
Y
2000
D, -X
(f)
UP, Y
PB 207.0C
100
X
-X
D, -Y
100

Fig. 4. Stereographic projections of cleaned directions determined by fitting least-square lines using LSA (Schmidt and Clark, 1985) to demagnetisation trends. Conventions are as for Fig. 1, with the exception of squares labelled 2 and 3 which are: squares labelled 2 are simply the relevant square 1 replotted after adding 180° to declinations (approximately with respect to geographic coordinates), and squares labelled 3 are the relevant square 2 replotted after restoring bedding to the horizontal. The directions marked with a cross are considered to be reversed directions and for the purpose of calculating a mean direction (squares marked 1) their anti-directions were combined with the normal directions (Note: for rocks this age assigning polarity is arbitrary but must be consistent once a convention is chosen).

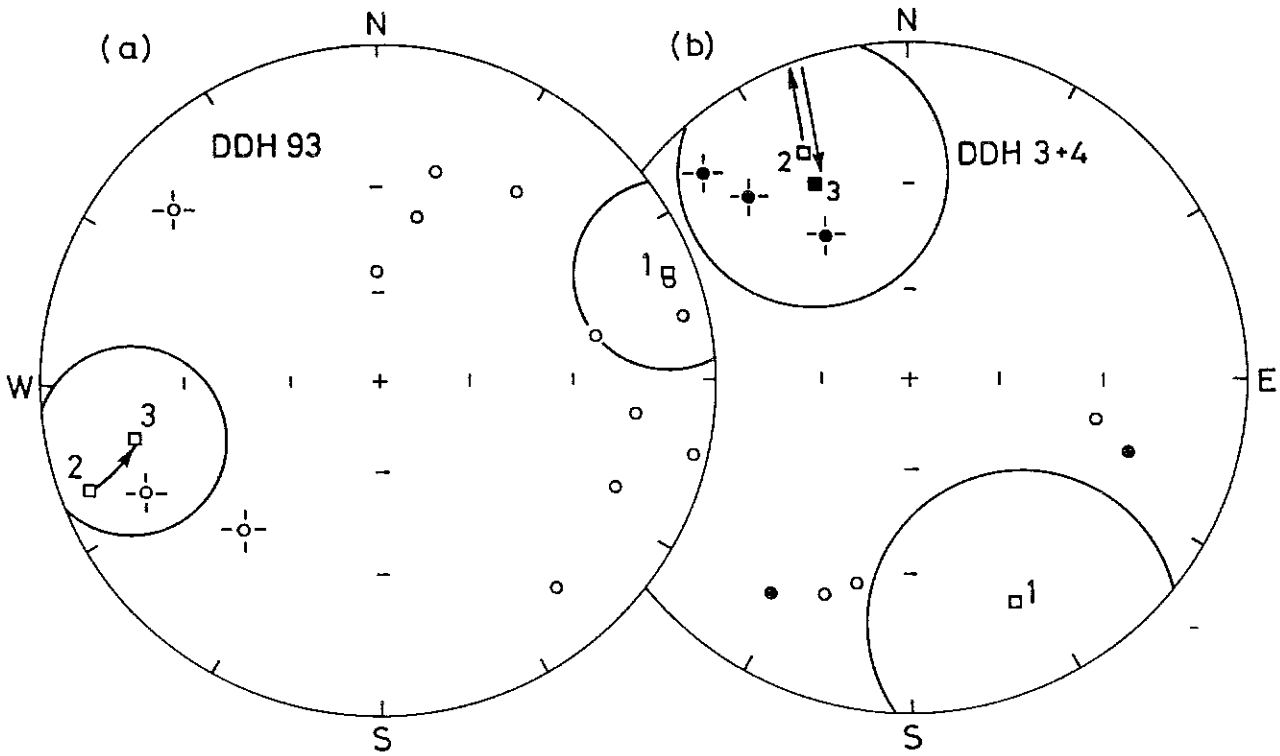
(a)
N
DDH 93
W
E
S
1
2
3
(b)
N
DDH 3+4
2
3
1
S

Fig. 5. Stereographic projections of all NRM directions from fully oriented block samples.

Conventions as for Fig. 1.

a) Tom Price - note tendency to a bimodal distribution, suggesting the presence of both normal and (almost) reversed magnetisations.

b) Paraburdoo - including samples from the Wyloo conglomerate which are plotted as squares, being conspicuously different from the other samples.

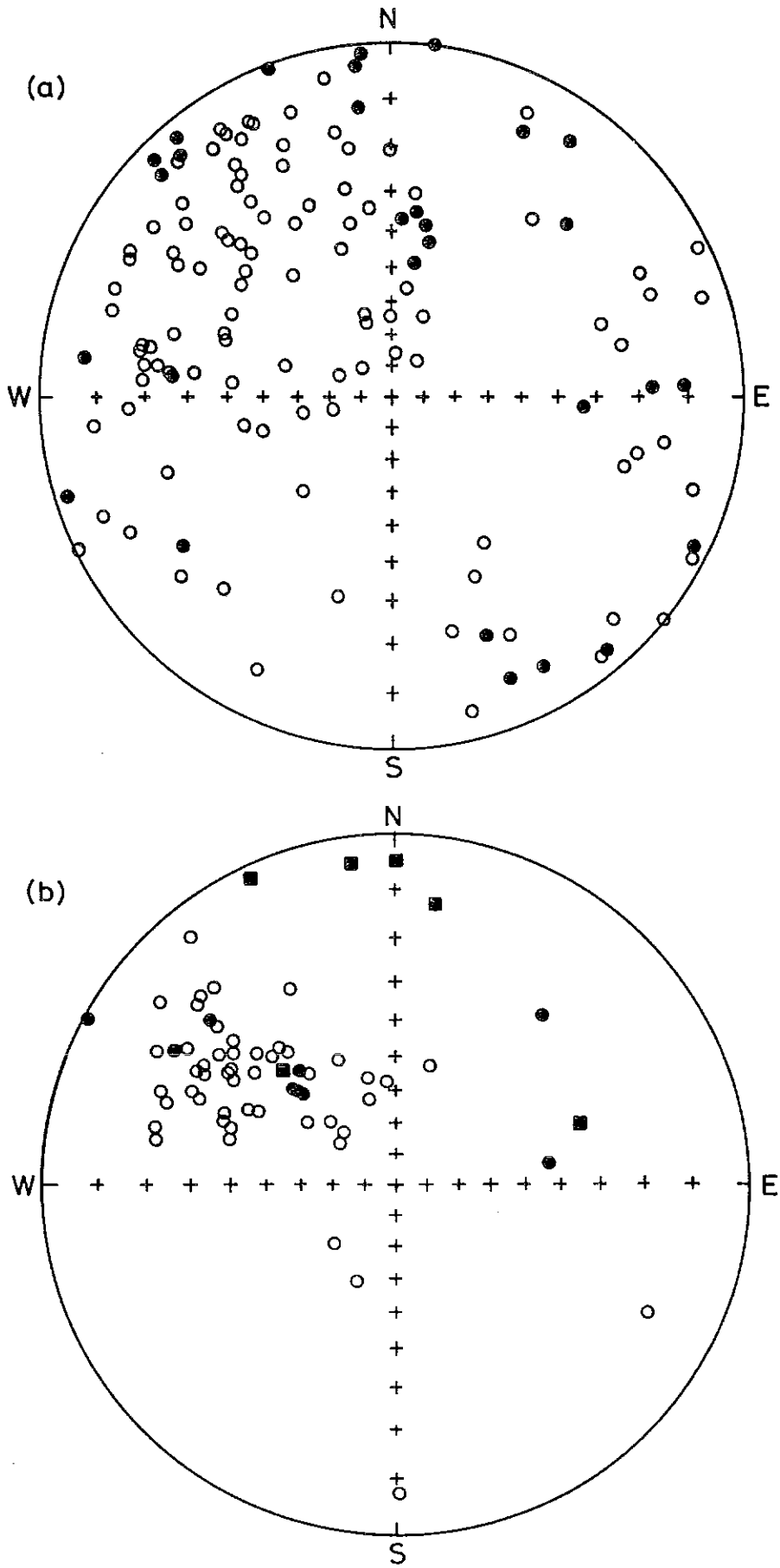
(a)
N
W
E
S
(b)
N
W
E
S

Fig. 6. Orthogonal projections of Paraburdoo block sample magnetisation vectors after various demagnetisation steps (conventions as for Fig. 3, except the horizontal plane is with respect to true north, true east, etc., since these directions are from fully oriented block samples). Demagnetisation steps following NRM are 10, 50, 100, 200 and 300 Oe AF, and 200, 300, 400, 500, 600, 670, 690°C.

a and b) Remarkably stable magnetisation from site PB 01, only decaying in intensity near the Curie temperature. The direction remains consistently north west and up.

c) Very stable magnetisation from site PB04, perhaps suggesting some second component near the Curie temperature, which remains unresolved before the intensity decays to zero. The major component is north west and up.

d) and e) As for a) and b) except these magnetisations are from site PB07.

f) Complex behaviour displayed only by samples from site PB 09 (The "Wyloo conglomerate") suggestive of individual clasts within samples possessing magnetisations with different directions and overlapping stabilities.

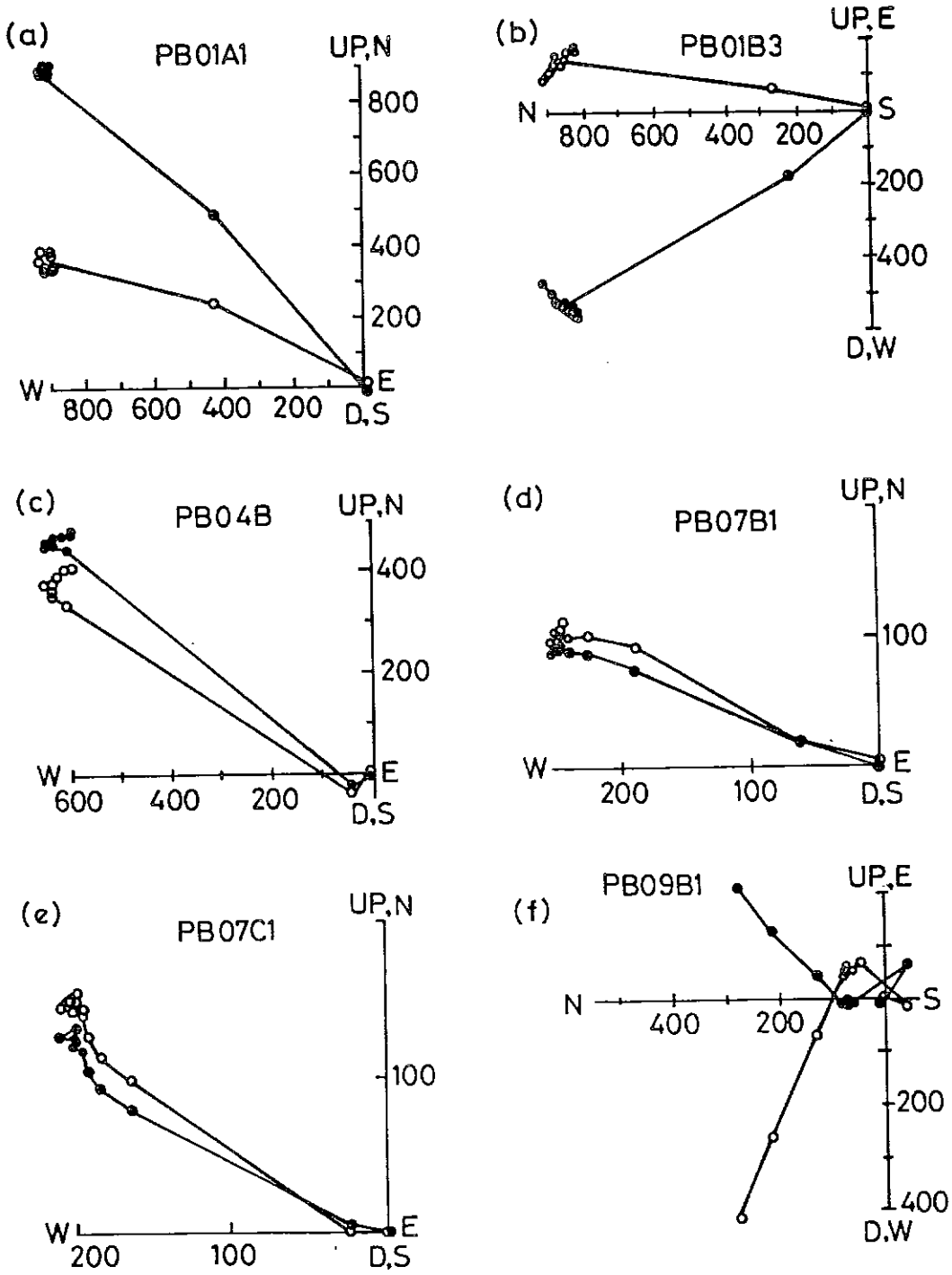
(a)
PB01A1
UP,N
800
600
400
200
W
800 600 400 200
E
D,S
(b)
PB01B3
UP,E
N
800 600 400 200
S
200
400
D,W
(c)
PB04B
UP,N
400
200
W
600 400 200
E
D,S
(d)
PB07B1
UP,N
100
W
200 100
E
D,S
(e)
PB07C1
UP,N
100
W
200 100
E
D,S
(f)
PB09B1
UP,E
N
400 200
S
200
400
D,W

Fig. 7. Stereographic projections of magnetisation directions determined after LSA (Schmidt and Clark, 1985), a least-squares fitting algorithm analogous to eye-balling "best" lines displayed by the orthogonal projections. Nevertheless many samples were dispersed and those have been indicated with a cross and rejected from calculation of the mean directions. It is emphasised that these directions have not been dismissed only because they do not conform, but in most cases also because of other peculiarities. In particular these are as follows:-

a) Paraburdoo - Sites PB 05 and PB 06 were very weathered (Marra Mamba) BIF with multi magnetic components present. Site PB 08 reveals normal and reversed tertiary directions, and may be also related to weathering.

b) Tom Price - all natural outcrops (especially Sites TP10 - TP14) show signs of weathering and/or lightning. Very high remanent intensities and Koenigsberger ratios are a diagnostic characteristic of lightning affected samples. These were very prevalent near the top of Mt. Nameless. TP06 was collected from Whaleback Shale which does not appear to be suitable for palaeomagnetic purposes (or at least would require much more intensive sampling). Samples TP 05B and TP 08C do not demagnetise towards the origin (e.g. Fig. 8c) indicating the presence of another magnetic component. Possibly reversals have been recorded by individual specimens. This aspect of the BIF at Tom Price could be investigated further although more fresh drill core samples would be required to avoid any ambiguity of weathering and lightning effects.

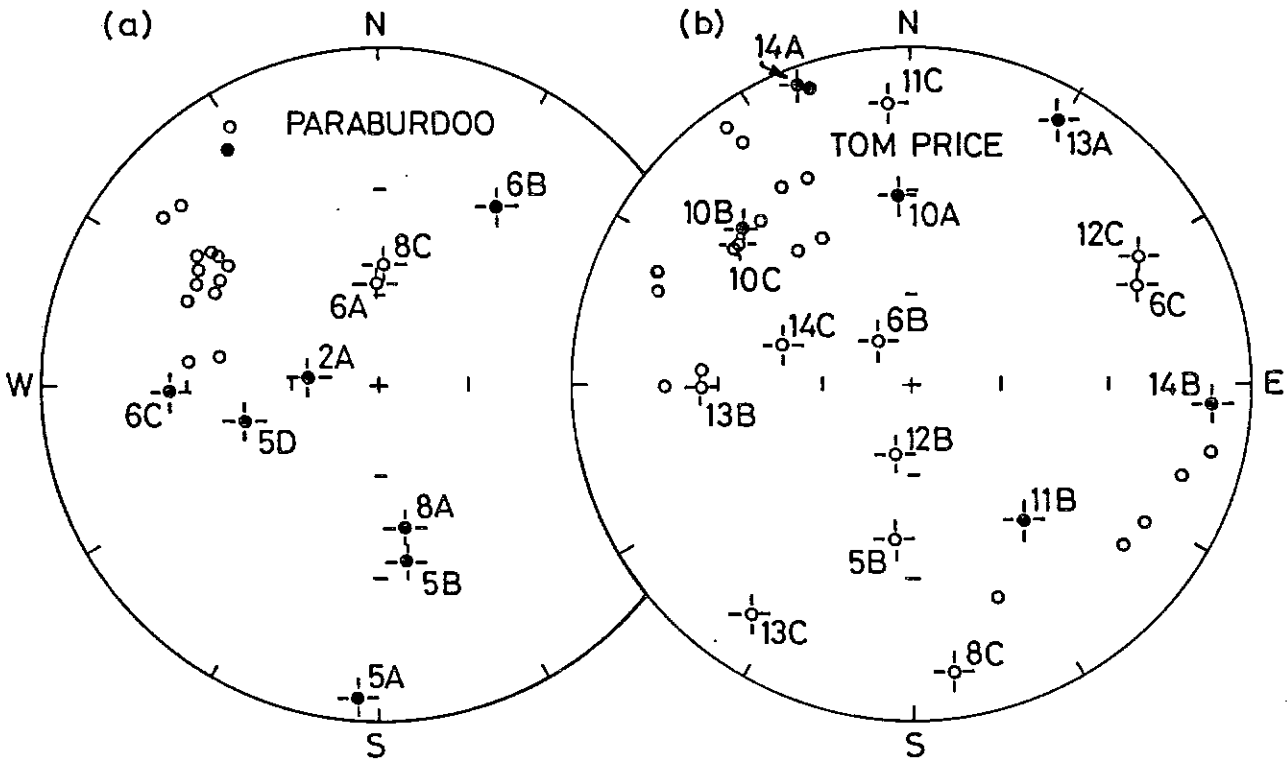
(a)
N
PARABURDOO
6B
8C
6A
2A
W
6C
5D
8A
5B
5A
S
(b)
N
14A
11C
TOM PRICE
13A
10B
10A
12C
10C
6C
14C
6B
13B
14B
E
12B
11B
5B
13C
8C
S

Fig. 8. Orthogonal projections of Tom Price block sample magnetisation vectors after various demagnetisation steps (conventions as for Fig. 6). Demagnetisation steps following NRM are 50 and 100 Oe AF, and 200, 300, 350, 400, 450, 500, 530, 560, 570, 580, 600, 630, 660 and 670°C.

a) Stable component of magnetisation from site TP03, directed WNW and up.

b) As for a) from TP 05A2

c) Also from site TP05, revealing underlying second magnetisation since the trend does not decay directly towards the origin, Note also that the direction is to the SE, or almost reversed as compared to b).

d) Another normal magnetisation from site TP05 (c.f. b and c), but not decaying directly to origin suggesting an underlying reversed (?) magnetisation.

e) and f) NW-up magnetisation from site TP09.

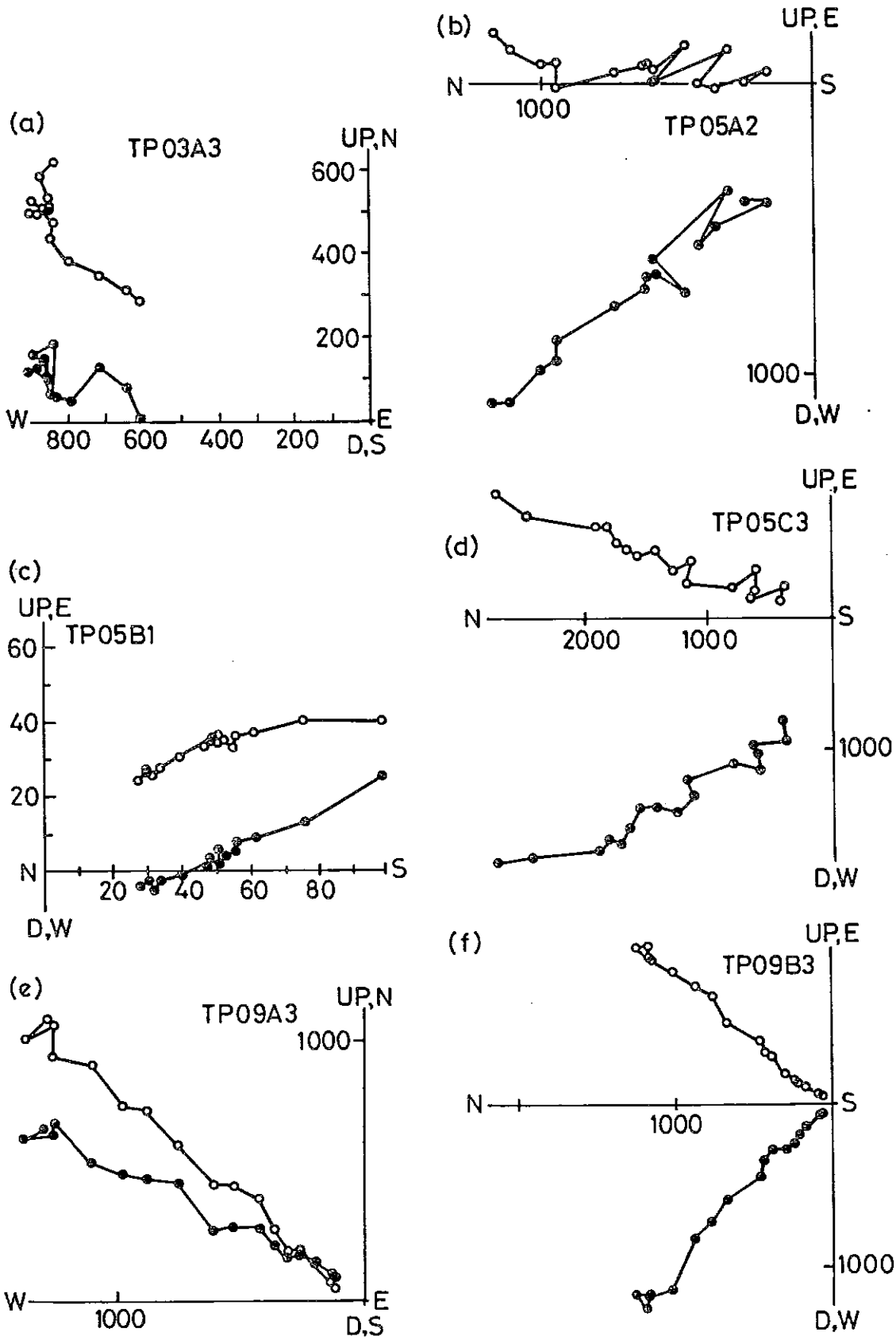
(a)
TP03A3
UP,N
600
400
200
W
800
600
400
200
E
D,S
(b)
UP,E
N
1000
S
TP05A2
1000
D,W
(c)
UP,E
TP05B1
60
40
20
N
20
40
60
80
S
D,W
(d)
UP,E
TP05C3
N
2000
1000
S
1000
D,W
(e)
TP09A3
UP,N
1000
W
1000
E
D,S
(f)
UP,E
TP09B3
N
1000
S
1000
D,W

Fig. 9. Stereographic projections of magnetisation directions from,

a) DDH 42 (circles - Dale Gorge Member) and DDH 44 (squares - Joffre and Weeli Wolli Members) after LSA (Schmidt and Clark, 1985) and

b) all areas investigated herein plus Dales Gorge and Joffre Members from Wittenoom (Embleton et al., 1979), comparing in situ directions with those after restoring bedding to palaeohorizontal. The error circles are for 95% confidence (α_{95} - Fisher, 1953) i.e. the true mean directions fall within these areas with 95% confidence. As discussed in Section 2.3 the magnetisations of the fresh BIF are pre-folding with 99^{+}% confidence. This can be appreciated by comparing the magnetisation directions from Paraburdoo BIF-DDH 42 + 44 (after unfolding the 56° and 60° south dipping limb) with those from Wittenoom BIF-WN (where beds are flat lying and require no unfolding). Other significant points are the close agreement between the BIFs and the Paraburdoo (PB) surface samples (after the latter are unfolded) and the poor agreement between the BIFs and the Tom Price (TP) surface samples (after unfolding and unplunging each site). This may indicate that the Paraburdoo surface samples were magnetised at virtually the same time as the BIFs were, although (as commented on the text) it should also be noted that the in situ PB magnetisations are indistinguishable from syn-deformational (Ophthalmian) magnetisations identified in the underlying Fortescue Group (JO, Fig. 10 and 11 - Schmidt and Embleton, 1985), suggesting a similar origin for the PB magnetisations. The TP magnetisations are also interpreted as being syn- or post-folding because their mean direction diverges slightly after structural restoration, and the directions scatter, reflected by the larger error circle associated with TP after unfolding (and unplunging).

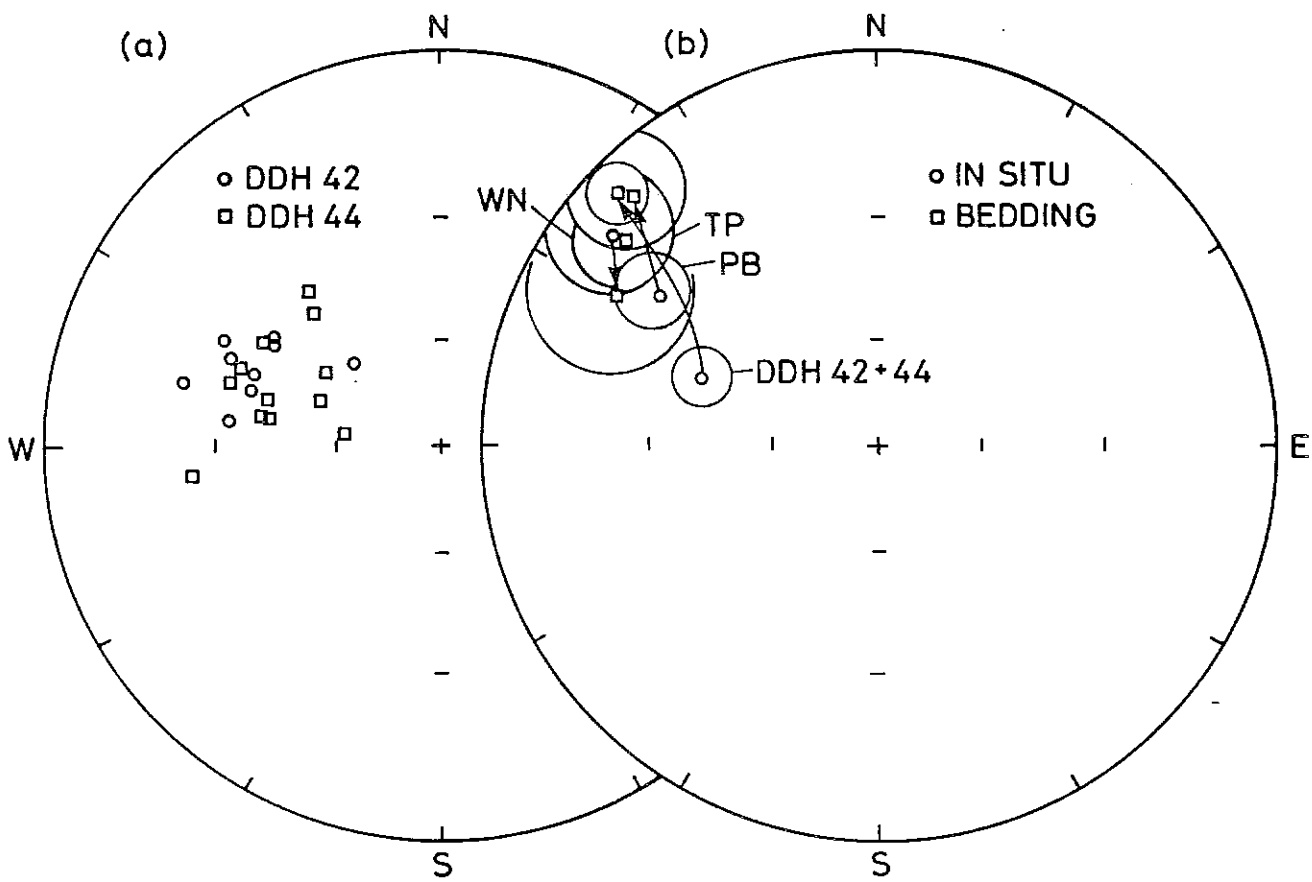
(a)
N
W
S
DDH 42
DDH 44
(b)
N
S
E
IN SITU
BEDDING
WN
TP
PB
DDH 42+44

Fig. 10 Precambrian apparent polar wander path (APWP) from Schmidt and Embleton, 1985. See Fig. 11 and Table 2 for symbols.

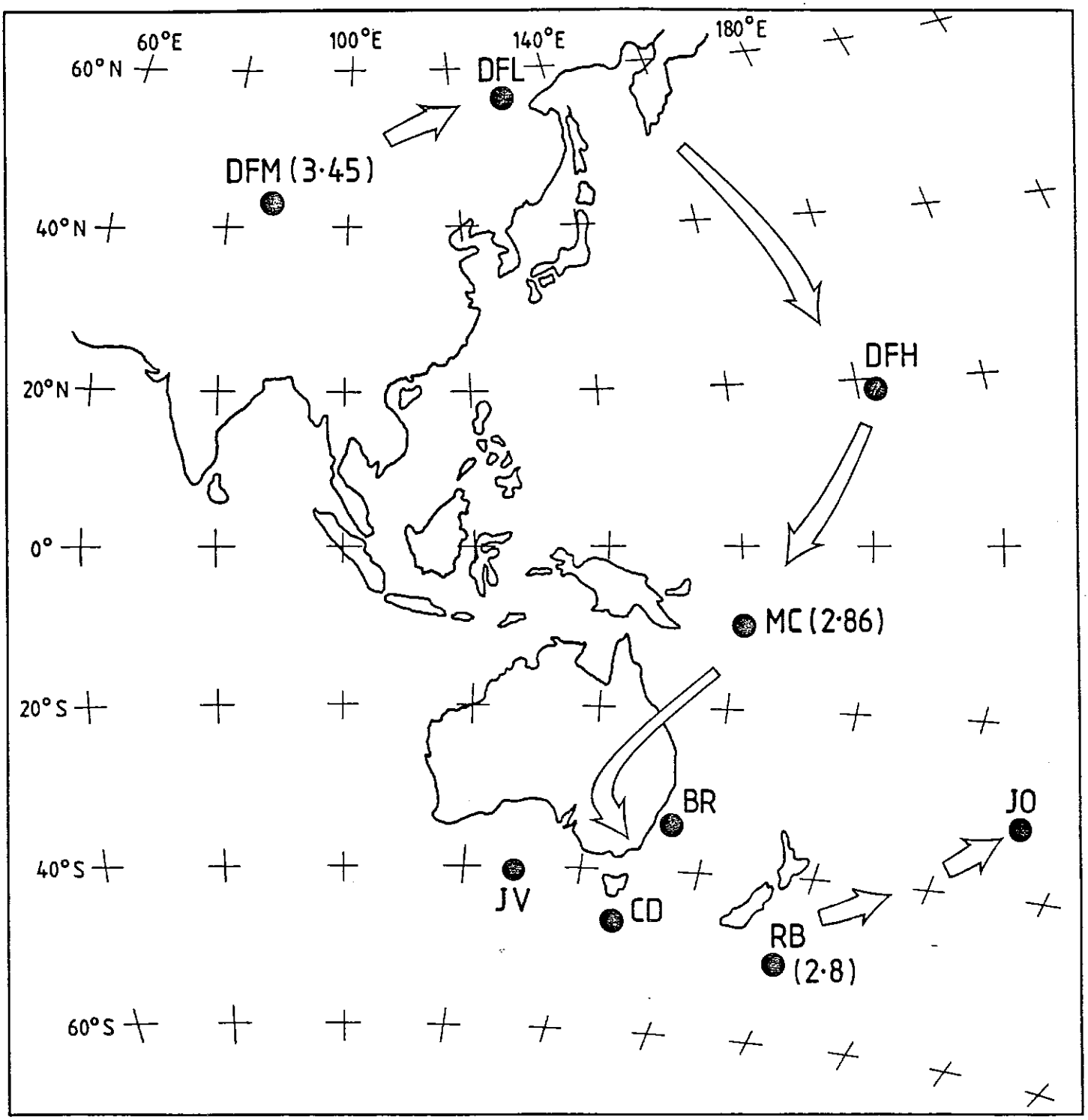
60°E
100°E
140°E
180°E
60°N
40°N
20°N
0°
20°S
40°S
60°S
DFL
DFM (3·45)
DFH
MC (2·86)
BR
JO
JV
CD
RB
(2·8)

Fig. 11. The Australian Precambrian apparent polar wander path (APWP) for times greater than 2860 My ago, until about 1800 My ago. The poles plotted are listed in Table 2. The two poles from the fresh BIF (PBA and WN) overlap and together are in close proximity to pole JO, representing the syn-deformational pole position from the Fortescue Group (Mt. Jope Volcanics - Schmidt and Embleton, 1985). Correction of the measured directions for the effects of anisotropy shifts the poles slightly towards RB. In addition, the poles from the (largely) mineralised samples (PBB and TPB) are also in this general vicinity. The figure shows these latter poles, with respect to present horizontal and with respect to palaeo-horizontal. Since the directions related to TPB tend to scatter after unfolding, a post-folding age is favoured for this pole. It is not clear, however, if PBB is pre- or post-folding because although it is indistinguishable from the overprint pole JO, it becomes indistinguishable from the pre-folding pole PBA when corrected for structural attitude (i.e. with respect to palaeohorizontal). Probably the most significant point to be made is that all the events from the initial magnetisation of the BIFs (deposition?), to folding and ore formation, appear to have occurred on a compressed time scale and/or little motion of the pole occurred from the time of initial magnetisation to the beginning of ore formation. It appears there may be a causal relationship between the onset of ore-formation and deformation. How long the ore-forming processes lasted may be reflected by pole position TPA, determined by Porath and Chamalaun (1968) which is significantly different from the equivalent pole (TPB) determined here and presumably reflects a real age difference within the Tom Price deposit. The Mt Newman ore seems to be similar in age to the younger Tom Price ore. All the magnetisations appear to be genuinely Precambrian in age and there is no suggestion of any Mesozoic or Tertiary components. The data suggest that the protore is related to the Ophthalmian Orogeny (~ 1800 My) with upgrading occurring at Tom Price and Mt Newman before ~ 1700 My, by which time the pole had moved to YF.

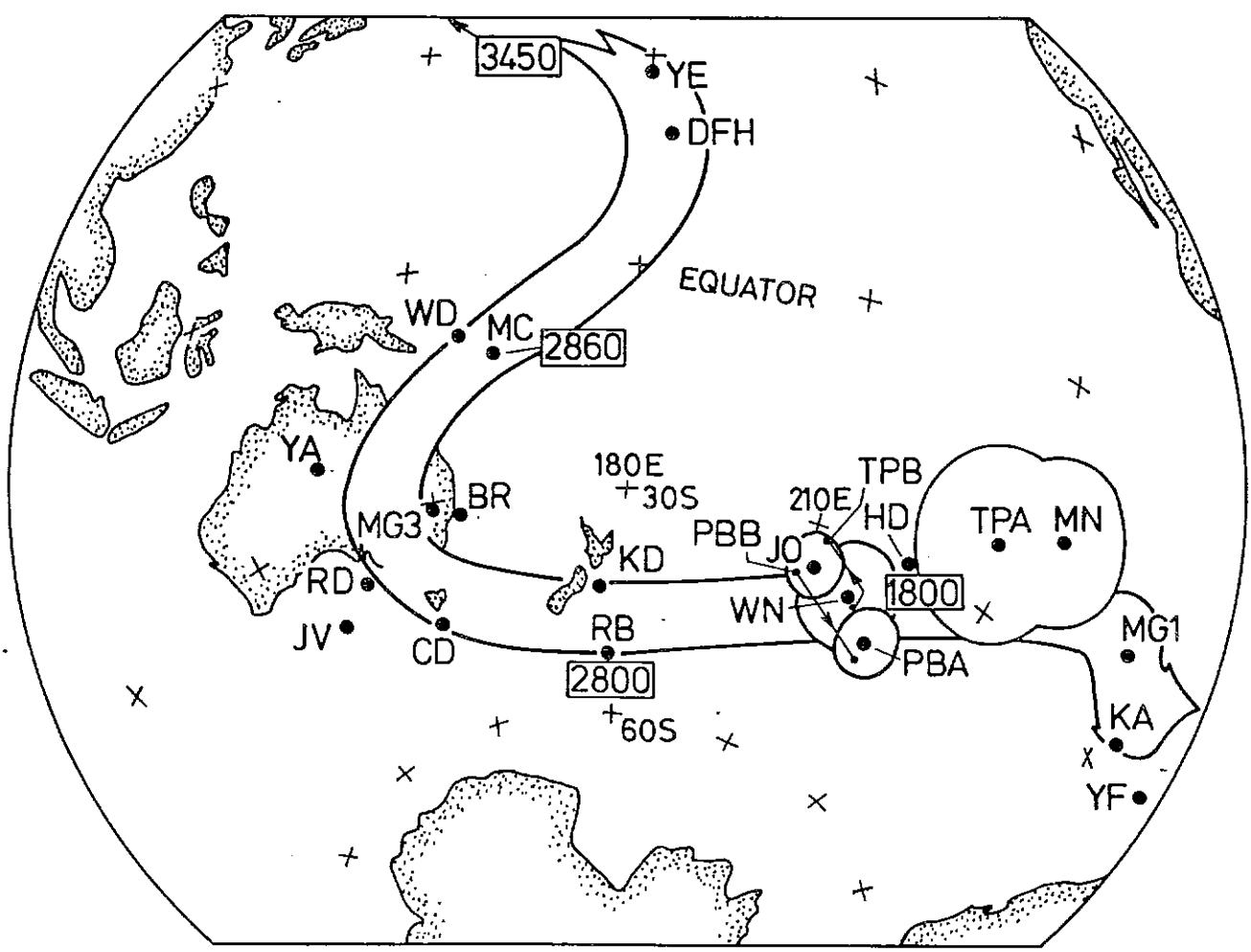
3450
YE
DFH
EQUATOR
WD
MC
2860
YA
180E
30S
TPB
210E
HD
TPA
MN
BR
MG3
PBB
JO
KD
RD
1800
WN
JV
CD
RB
MG1
PBA
2800
60S
KA
YF

Fig. 12 Susceptibility (χ) variations with temperature are performed using the CSIRO transformer - bridge (Ridley and Brown, 1978) in conjunction with a small furnace. Diagnostic features are (see main text for details) -

a) the isotropic point (-150°C), characteristic of multi-domain (MD) magnetite,

b) the Morin transition (-20°C) indicating the presence of coarse crystalline haematite, and

c) The Hopkinson peak immediately preceding the disappearance of susceptibility, reflecting the presence of optimum sized magnetic grains for palaeomagnetic studies. The Curie temperature for magnetite is 580°C, for α-haematite, 680°C and for cation deficient magnetite (kenomagnetite), variable but often observed at about 610°C.

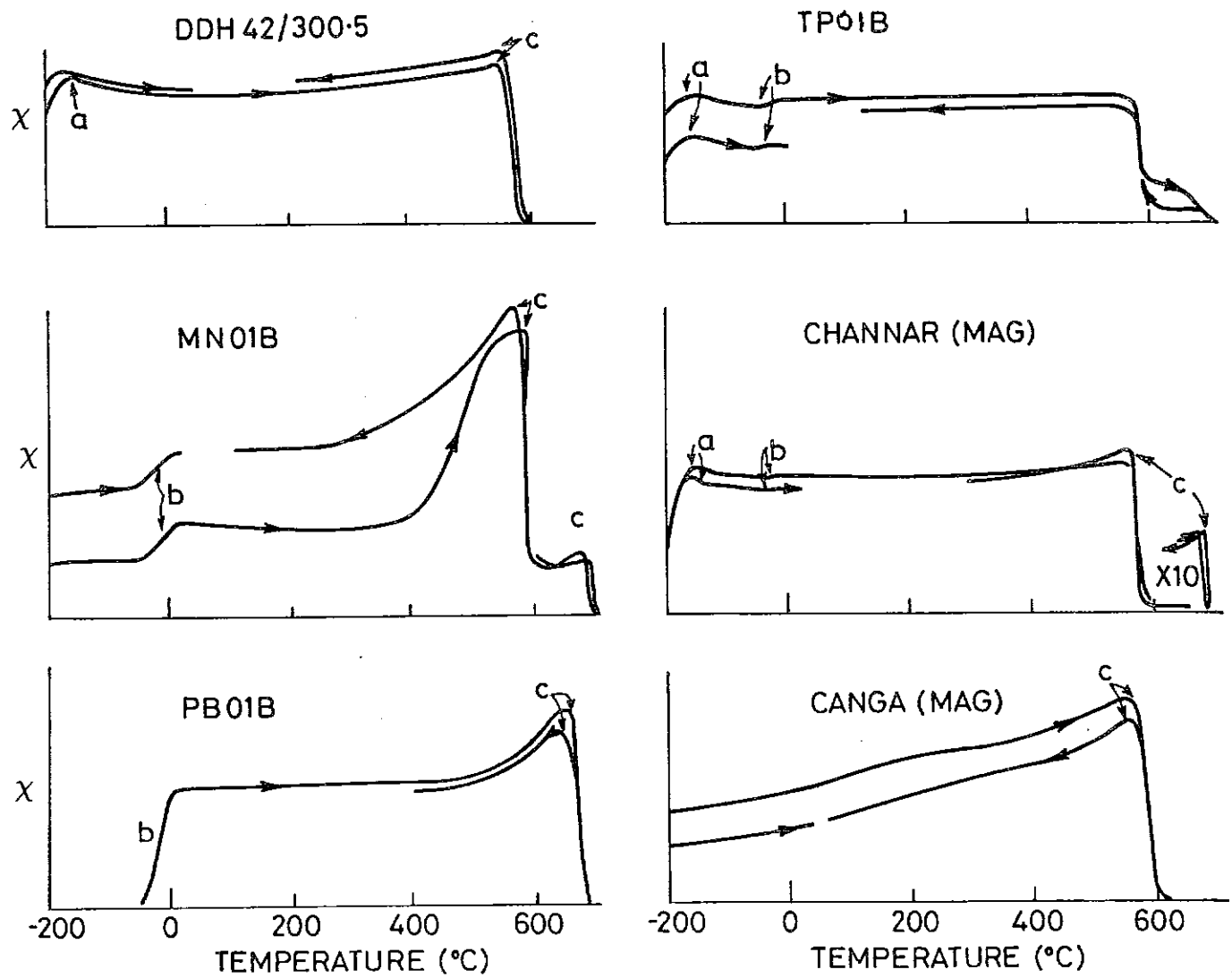
DDH 42/300·5
χ
a
c
TP01B
a
b
MN01B
χ
b
c
c
CHANNAR (MAG)
a
b
c
X10
PB01B
χ
b
c
CANGA (MAG)
c
-200
0
200
400
600
TEMPERATURE (°C)
-200
0
200
400
600
TEMPERATURE (°C)

APPENDIX I - SAMPLING SITES

A. TOM PRICE MINE AREA	DESCRIPTION
TP01 Synclines, Minor fold, Southern Batter Fault 890 Bench, Plunge 9° to W Bedding 55° to 030°	Some veining Oxidised Dales Gorge
TP02 N.W. Deposit, Band 7, 780 Bench, Bedding 11° to 311°	Dales Gorge BIF
TP03 N.W. Deposit, Band 10, 11 (Bedding 7° to 008°) and 12 Bedding 17° to 201°), Plunge 13° to W	Mineralised Dales Gorge
TP04 Synclines, 885 Bench, Bedding 44° to 191°, Plunge 10-20° to W	Leached Joffre BIF
TP05 Synclines, 885 Bench, Band 17, Bedding 30° to 030°, no plunge	Dales Gorge BIF
TP06 30 mE of TP05	4 m "Wavy" BIF in Whaleback Shale
TP07 Natural outcrop, north wall, about 830 Bench, Bedding 48° to 10°	Dales Gorge BIF
TP08 Synclines, 870 Bench, Bedding 66° to 207°	Microplaty He ore
TP09 Section 6, Bedding 40° to 264°	Dales Gorge Martite (He) goethite
TP10 Airport rd. behind Mt Nameless, Bedding 30° to 330°	Lowermost Dales Gorge, oxidised BIF
TP11 Along track to top of Mt Nameless (off old Paraburdoo Rd), Bedding 38° to 038°	Bruno's band BIF (just below Dales Gorge)
TP12 Towards top of Mt Nameless, just below Hamersley Surface, Bedding 09° to 339°	Dales Gorge BIF
TP13 Bulldozed track near top of Mt Nameless, Bedding 10° to 348°	Joffre BIF
TP14 100 m down track from TP13	Joffre BIF

CORE SAMPLES	DESCRIPTION
DDH ND93/80	
172.4 m	BIF85GY/SHL10GN/CAR5
	(near top DG)
179.6 m	BHM95GY/H2F5
174.2 m	BHM100GY
184.8 m	BHM90GY/H2M10
188.3 m	BHM95GY/H2F5
200.0 m	H2H 100GY
227.6 m	BIF90GY/H2H10
230.5 m	H2H100GY
235.2 m	BHM100GY
237.2 m	BIF100GY
240.5 m	SHL 100 GN
242.3 m	H2H85GB/SHF15
245.9 m	Interbedded shale and magnetic H2H
249.9 m	Magnetic H2M + Dolomite
251.0 m	Magnetic H2M + dolomite

B. PARABURDOO MINE AREA	DESCRIPTION
PB01 11 Bench North 4E, Band 12, Bedding 46° to 214°	Dales Gorge H2M ore
PB02 Same face as PB01, J2 Strand Bedding 36° to 200°	Joffre H2H ore
PB03 11 Bench NW, J2? Bedding 44° to 186°	Joffre H2H ore (more goethitic than PB01-01)
PB04 Same as PB03, J2? Bedding 36° to 190°	Oxidised Joffre BIF
PB05 Drum Corner, ~1000E Bedding 30° to 190°	Lower Marra Mamba oxidised BIF
PB06 Western 45, ~600E Bedding 56° to 199°	Upper Marra Mamba (Haematitic)
PB07 13 Bench NW, Bands 13 and 14, 800E, Bedding 52° to 207°	Oxid. Dales Gorge BIF
PB08 14 Bench, Band 7? 600E	Dales Gorge H2H
PB09 1 km S of 4 W 52° to 207°	Wyloo conglomerate

CORE SAMPLES DDH42/depth (m)	DESCRIPTION
42/207.0	Top of Dales Gorge, Grey BIF with riebeckite (v.mag)
42/220.0	B15 grey wall-banded BIF (magnetic)
42/234.8	B14 grey BIF, much haematite (strongly magnetic)
42/261.5	B12 BIF with rare red oxidised bands (str. mag.)
42/284.7	B9 grey to greenish grey BIF, numerous red oxidised bands (str. mag.)
42/300.5	B8 grey to green BIF (magnetic)
42/326.2	B3 dark grey BIF, veins of pyritic calcite and quartz
42/354.7	B2? Mt dominant laminated BIF
42/379.8	B1? BIF chert dominant BIF

4E DDH44/depth (m)	DESCRIPTION
44/49.8	Weeli Wolli cherty strongly leached and oxidised
44/121.0	Weeli Wolli magnetic BIF
44/129.0	" " " "
44/160.3-.5	BIF/Dolerite contact, Grey to reddish Mt, well banded BIF, minor riebeckite
44/174.8-5.2	BIF/dolerite contact. Grey to light grey BIF, magnetic.
44/184.4	Coarse mesobanded dark grey to light grey magnetic BIF with abundant riebeckite.
44/224.9	Moderately magnetic BIF, abundant riebeckite
44/251.2	Bluish grey moderately magnetic well mesobanded BIF
44/276.5	Finely laminated greenish to blue/grey magnetic BIF
44/290.4	Riebeckite BIF with magnetite
44/312.5	Grey to bluish grey BIF, J1

18E DDH3/depth (m)	Marra Mamba ore
3/7.7, 11.5, 20.4, 29.0, 59.5, 71.3	
18E DDH4/depth (m)	Marra Mamba ore
4/39.1, 41.0, 44.6	(magnetic)

APPENDIX II - DDH ORIENTATION

The use of remanent magnetisation for independently orienting drill core has been discussed by many workers (Lynton, 1938, Fuller, 1969, Henry, 1982 and Kodama, 1984). Lynton (1938) advocated simply using the natural remanent magnetisation (NRM) direction, since the multiple component nature of NRM had not then been fully appreciated and in any case, cleaning methods had not been developed, while Fuller (1969) and Kodama (1984) describe the use of thermal and/or alternating field (AF) cleaning to determine that part of the NRM which has been acquired in the recent geomagnetic field, that is, the viscous remanent magnetisation (VRM). Knowledge of the direction of VRM allows drill cores to be azimuthally oriented (except, of course, if the drill hole and the geomagnetic field are aligned). Henry (1982) briefly reports using "cleaned" primary magnetisation directions to orient drill cores. This method can be used when the age of a rock is known and the relevant segment of the apparent polar wander path has been established. Both Henry (1982) and Kodama (1984) mention drilling induced secondary magnetisation which detracts from using the VRM component (1982) for azimuthal orientation, although Henry (1982) uses the consistent polarity of the induced magnetisation to reasign the facing of some core pieces that had inadvertently been placed in drill trays the wrong way.

DDH 42 and 44 from Paraburdoo were selected for sampling not only because they penetrated fresh BIF (Dales Gorge, Joffre and Weeli Wolli) but also because of the consistent regional southerly dip. The bedding attitude in itself enables the drill core to be oriented azimuthally and affords any other attempts to orient the drill core with a cross reference. Magnetisation directions from drill core material sampled for this study were measured with respect to the apparent down dip direction, which at Paraburdoo is southerly. Simply adding 180° to the measured declination angles should give an approximation to the in situ magnetisation directions, because the drill holes are almost vertical (the proper correction is more refined for drill holes that diverge from verticality, and is dealt with below). The NRM directions of samples from DDH42 and 44 are plotted in Fig. 1a, and are discussed in Section

2.1. Of particular note is the rather good grouping displayed by NRMs from samples of DDH 44, while the NRMs from samples of DDH 42 are scattered.

Preliminary AF cleaning (Fig. 2a) of DDH 42 samples showed the source of scattering to be soft overprints, but not in the expected direction of a VRM due to the geomagnetic field. In fact the magnetic components present in these samples (both original and overprint) are closely constrained to the bedding plane. It has been shown by simple laboratory experiment that the soft overprints present in DDH 42 are most probably related to magnetic logging and sample preparation (drilling and slicing). Fig. A2.1 shows intensity changes induced in three specimens during abrasive polishing of their bottom ends S_1, S_2 and S_3. Also shown in this figure is the growth of viscous magnetisation (V_1, V_2 and V_3) in different orientations in the Earth's field which is insignificant compared to the polishing induced mangetisation. The 20mT AF demagnetisation steps interspersed between the other steps shown in Fig. A2.1 show that both the viscous and polishing induced (piezomagnetic) magnetisations are soft and are easily eradicated. Of greater significance is the chemical demagnetisation step (c), which involved immerson of the specimen bottoms in 10N HCl for 50hr and quite clearly demonstrates that the polishing affects the magnetisation of external grains only. The BIF is not porous enough to allow significant acid penetration in 50hr. It was concluded that although pristine Dales Gorge BIF (DDH42) possibly carries a small VRM component, the effects of drilling, logging and sample preparation introduce extraneous components that reset the VRM, rendering this component of the NRM indeterminable. Dales Gorge BIF does possess, however, a harder magnetisation which is consistent in direction and may be used to orient drill core as discussed below.

The NRMs of Joffre and Weeli Wolli BIF are well grouped, suggesting the dominance of a single magnetic component. In itself this would not eliminate the detection of other components present, although it would be expected that they would be much smaller than this main component. The most sensitive method for determining VRM components is continuous thermal demagnetisation (Schmidt and Clark, 1986). Six

specimens from DDH 44 containing predominantly magnetite or predominantly haematite were subjected to this method. No magnetic components with a direction of that expected from VRM were found however, confirming the initial suggestion that the Joffre and Weeli Wolli BIF possess essentially single magnetisation components. In fact these samples proved to be remarkably stable to thermal demagnetisation, with reversible changes in intensity occurring up to near the Curie Temperature. This is illustrated in Fig. A2.2 where measured intensities for two specimens from DDH 44 (one containing mainly magnetite (Mt) and another only haematite (Ht) are compared with the reversible change of saturation magnetisation (J_s) with temperature. It is apparent that overall the measured points and the $J_s(T)$ curves for both magnetite and haematite are coincident. Small departures below 100°C showed no consistency of direction and although their origin is uncertain they are unlikely to be related to any VRM component which, if present, ought to be discernible up to 300°C for magnetite and 400°C for haematite. VRM components were not detected using step-wise thermal demagnetisation either (c.f. DDH 44 NRM Fig. 1a and cleaned oriented directions Fig. 9a) supporting the results from the continuous demagnetisation. There seems to be little prospect, therefore, of utilising VRM to orient BIF drill core samples. However, the stable portions of the NRMs determined from both thermal and AF demagnetisation (Section 2.1) are consistently directed to the north-west, with low negative inclination after using bedding attitude to orient drill cores (see below), and restoring bedding to the palaeohorizontal. This latter correction is justified by the fold-test described in Section 2.3. Thus it is proposed that the stable portion of NRM in the fresh BIFs may be independently used to orient DDH samples.

To fully realise the potential of the remanent magnetisation measurements herein, drill cores have been oriented using bedding attitudes which are southerly for DDH 42 and 44. If these drill holes were vertical, then a simple addition of 180° to declinations (herein measured with respect to apparent down dip azimuth - for drill core samples) would express magnetisation directions with respect to geographic coordinates. This is in fact done for DDH 93/80 (Tom Price),

DDH 3 and 4 (Paraburdoo), where the assumptions of consistent bedding attitudes may be invalid (see main Text). For DDH 42 and 44 errors incurred assuming a consistent bedding attitude, and verticality of drill holes are small. Consequently, it was considered desirable to develop a method to handle divergence from verticality of drill holes.

Consider a non-vertical drill hole that intersects strata of known attitude. It is clear that, providing the bedding plane and correct facing can be identified in the drill core sample, there is a unique solution for determining the sample's orientation. The problem is not trivial however, because the apparent down dip azimuth (as determined by viewing the drill core) will not in general coincide with the real down dip azimuth. Only when the drill hole is vertical will the two coincide. The bedding pole is the only immutable parameter. The other parameters required to determine the orientation are the drill hole azimuth and plunge.

We are required to find ε (Fig.A2.3), the rotation of the specimen about the DDH axis which brings the bedding into alignment with the regional strike. The bedding has R→L strike α and dip δ.

$$\therefore \mathbf{n} = (\sin\alpha \sin\delta, -\cos\alpha \sin\delta, -\cos\delta)$$
$$\mathbf{i} = (\cos\varepsilon \sin\Delta, \sin\varepsilon, -\cos\varepsilon, \cos\Delta)$$

$$\mathbf{k} = (\cos\Delta, 0, \sin\Delta)$$
$$\therefore \mathbf{n} = \mathbf{i}\sin\delta' - \mathbf{k}\cos\delta'$$
$$= (\cos\varepsilon \sin\Delta \sin\delta' - \cos\Delta\cos\delta', \sin\varepsilon\sin\delta', -\cos\varepsilon\cos\Delta\sin\delta' - \sin\Delta\cos\delta')$$

Equating strikes:

$$-\cot\alpha = \frac{\sin\varepsilon \sin\delta'}{\cos\varepsilon \sin\Delta \sin\delta' - \cos\Delta\cos\delta'}$$

$$\therefore \tan\alpha = \cot\delta' \cos\Delta \operatorname{cosec}\varepsilon - \sin\Delta\cot\varepsilon$$

$$\sin^2\varepsilon \left[1 + \frac{\sin^2\Delta}{\tan^2\alpha}\right] - \frac{2 \cot \delta' \cos \Delta}{\tan \alpha} \sin \varepsilon + (\cot^2\delta' \cos^2\Delta - \sin^2\Delta)/\tan^2\alpha = 0$$

$$\therefore \sin \varepsilon = \frac{2\cot\delta'\cos\Delta\tan\alpha - \sqrt{[4\cot^2\delta'\cos^2\Delta\tan^2\alpha - 4(\tan^2\alpha+\sin^2\Delta)(\cot^2\delta'\cos^2\Delta-\sin^2\Delta)]}}{2(\tan^2\alpha + \sin^2\Delta)}$$

Calculation of local dip - only the strike of the regional bedding has been used so far, thus the local dip can be calculated to compare with the regional dip.

Equating z components of n

$$-\cos \delta = -\cos \varepsilon \cos \Delta \sin \delta' - \sin \Delta \cos \delta'$$
$$\cos \delta = \sin \Delta \cos \delta' + \cos \Delta \sin \delta' \cos \varepsilon$$

Fig. A2.1 Remanent intensity variations of three DDH 42 specimens following various treatments. The 20mT refers to AF demagnetisation in a peak AF of 20mT (200 Oe).

V_1, V_2 and V_3 refer to viscous acquisition of remanence in the Earth's field for 24 hrs in an upright orientation, for 10 minutes upside down followed by 1hr upright, respectively. S_1, S_2, S_3 refer to abrasive polishing (simulating slicing) of the ends of specimens in the laboratory field near the slicing machine (Earth's field plus anomalous field due to approximately 1 tonne mass of iron) in upright orientation, upside down and upright again respectively (the direction of magnetisation of the middle polishing induced magnetisation S_2 was approximately reversed compared to S_1 and S_3). C refers to chemical demagnetisation of specimen ends in 10N HCl for 48 hrs. The purpose of these tests was to investigate the source of anomalous natural remanent magnetisation (NRM) directions in DDH 42. It was concluded that both hand magnets and sample preparation (drilling and slicing) probably contributed to the scattered directions, producing spurious IRM and piezomagnetic components respectively, and that while AF demagnetisation enables the original direction to be retrieved (at the expense of partially demagnetising the specimens and losing information on original intensities), chemical demagnetisation of the affected surface grains should allow the intensity of magnetisation to be retrieved as well if drilling and slicing was the sole cause.

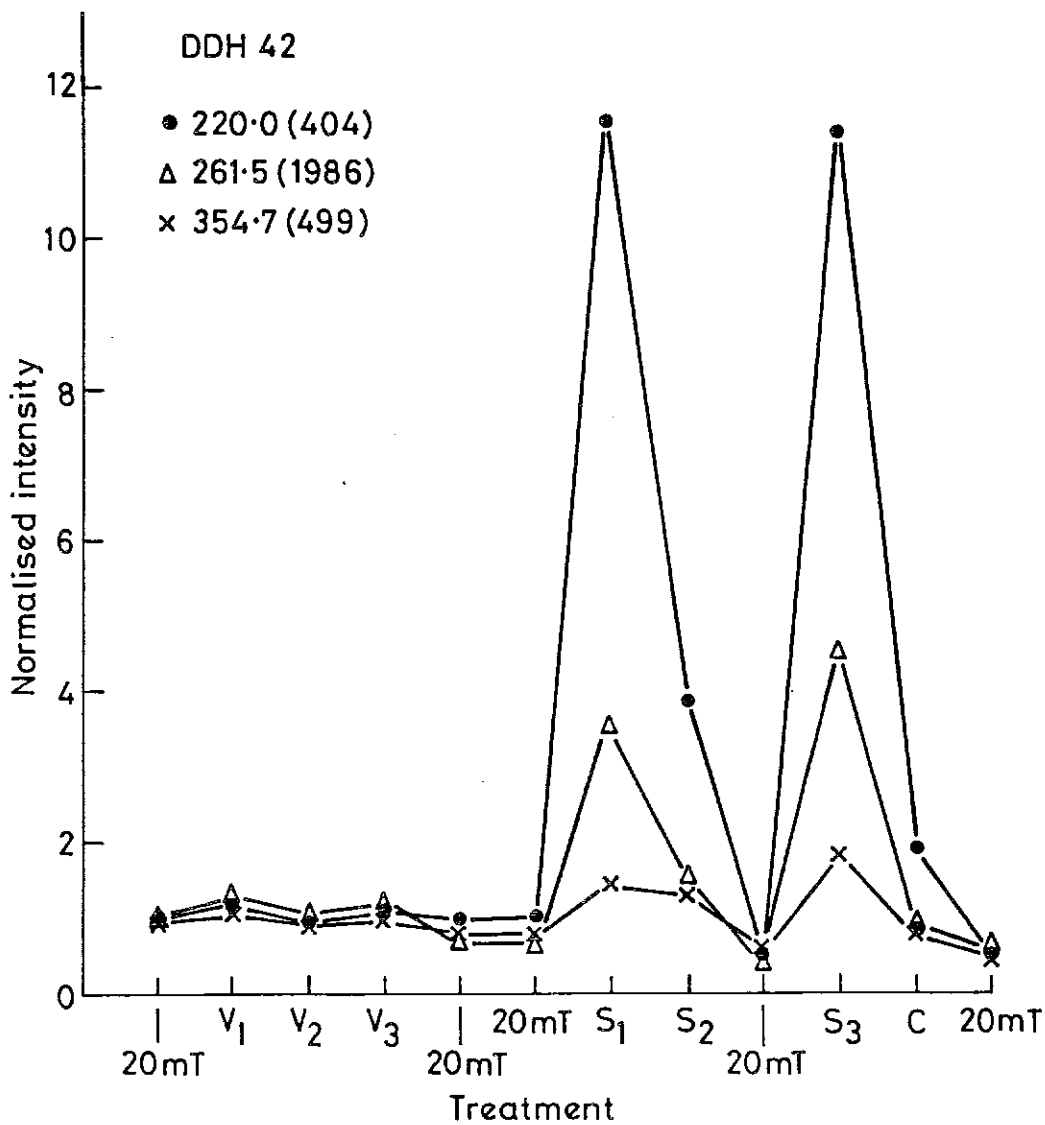
DDH 42
● 220·0 (404)
Δ 261·5 (1986)
× 354·7 (499)
Normalised intensity
0
2
4
6
8
10
12
20mT
V1
V2
V3
20mT
20mT
S1
S2
S3
C
20mT
Treatment

Fig. A2.2. The data points (dots) represent magnetic remanence monitored continuously with temperature using the modified DIGICO continuous heating magnetometer. The curves represent the expected change in saturation magnetisation (J_s) of magnetite (Mt) and haematite (Ht) i.e. the decrease due to thermal agitation only. J_s/T curves are reversible, unlike remanence which after unblocking no longer contributes to the signal on cooling. The coincidence of the measured remanence and the standard Js/T curves for the DDH 44 samples shows that no unblocking takes place until immediately before the Curie points. There are no magnetic grains present in DDH 44 of a grain size/shape suitable for acquiring viscous remanent magnetisation (VRM). VRM can not therefore be used to orient this BIF drill core. The remarkable stability of the ancient remanence has, however, ensured its survival since acquisition, and this can be used to independently orient BIF cores.

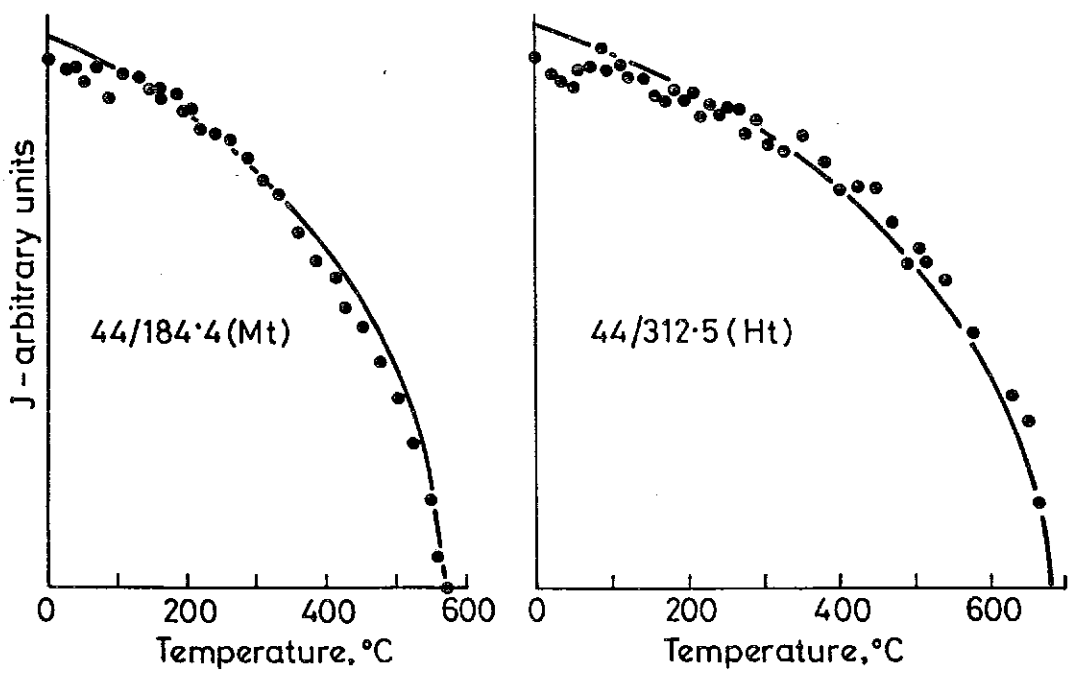
J - arbitrary units
44/184·4 (Mt)
0
200
400
600
Temperature, °C
44/312·5 (Ht)
0
200
400
600
Temperature, °C

Fig. A2.3 Geometry of DDH orientation

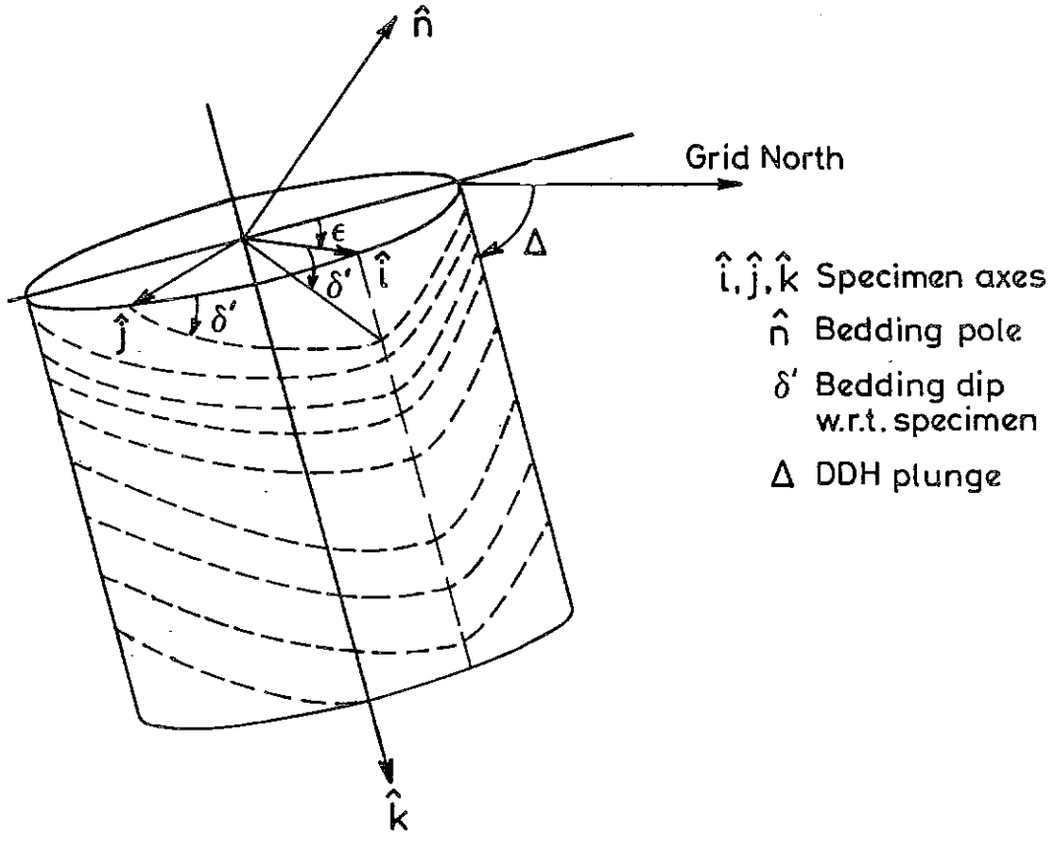
n̂
Grid North
ε
Δ
δ'
î
ĵ
δ'
k̂
î, ĵ, k̂ Specimen axes
n̂ Bedding pole
δ' Bedding dip w.r.t. specimen
Δ DDH plunge

APPENDIX III. Local Magnetic Declinations

Site	Local declination		Declination anomaly
TP01	0°		-1°
TP02	1°		0°
TP03	-4°		-5°
TP04	-2°		-3°
TP05	-3°		-4°
TP06	-2°		-3°
TP07	-5°		-6°
TP08	0°		-1°
TP09	-5°		-6°
TP10	-15°		-16°
TP11	1°		0°
TP12	-23°	(-80° to +31°)	-24°
TP13	-79°	(-175° to 51°)	-80°
TP14	5°	(-9° to +19°)	+4°
PB01	6°		+5°
PB02	6°		+5°
PB03	5°		+4°
PB04	5°		+4°
PB05	5°	(-5° to +12°)	+4°
PB06	1°	(-26° to +30°)	+0°
PB07	1°		0°
PB08	1°		0°
PB09	-4°		-5°

All declinations are positive E of N.

The local declination for each site is the average of three or four differences between sun (true) azimuths and magnetic azimuths. The regional (IGRF) declination for the area is +1°.